Lithium Ion Battery Cell Modelling

By

Hamdihun Abdie Dawed

Submitted to the Department of Electrical Engineering, Electronics, Computers and Systems

in partial fulfillment of the requirements for the degree of

Erasmus Mundus Master Course in Sustainable Transportation and Electrical Power Systems

at the

UNIVERSIDAD DE OVIEDO

August 2017

Author . . . .

Certified by. . . . .

Associate Professor

Thesis Supervisor

Certified by. . . . .

Associate Professor

Thesis Supervisor

Lithium Ion Battery Cell Modelling

By

Hamdihun Abdie Dawed

Submitted to the Department of Electrical Engineering, Electronics,

Computers and Systems

in partial fulfillment of the requirements for the degree of

Erasmus Mundus Master Course in Sustainable Transportation and Electrical Power Systems

Abstract

In this thesis, a lithium ion battery cell is analyzed and modelled on MATLAB. Under lithium ion battery there are different chemistries. The electrical and thermal performance of each chemistry varies depending on the operating conditions. Developing a model of performance which accounts the current rating, operating temperature and state of charge (SoC) helps to analyze the behavior of the cell under load. Different approaches of modelling lithium ion battery cells are proposed in literature, physics based electrochemical model and empirical (such as equivalent circuit-EEC model) are the most discussed. In this work, empirical based EEC model is designed and simulated for various working conditions. The model has a variable voltage source which accounts the open circuit voltage (OCV) as a function of state of charge and temperature, a series resistor to account the instantaneous voltage change when the cell is under load or relaxed, and parallel resister-capacitor (RC) branches to capture the dynamics of the cell during transient. The battery cell is exercised under different current rate, state of charge and temperature; and data is recorded for impedance parameters identification. Curve fitting techniques are applied to determine the number of RC branches. Two/Three RC branches are chosen based on a trade-off between fitting goodness of the transient characteristics of the selected battery cell and the parameter identification complexity. Trust-Region-Reflective method based on least square algorithm on Simulink optimization toolbox is used to identify the parameters (resistor and capacitor as a function of temperature, current rate and SoC). The cost function in the optimization problem is sum squared error of the terminal voltage. The estimated parameter values are highly nonlinear and represented in the model by 3D lookup tables with linear interpolation. Coulomb counting method is applied to estimate SoC which considers temperature dependent maximum capacity of the cell. OCV is modelled in terms of 2D lookup table with smooth interpolation, as a function of SoC and

temperature, from measurement data using pulse charge-discharge technique with 1-hour relaxation time. Once the impedance parameters are estimated, OCV model is improved by estimating new data points to handle the limitation of coulomb counting SoC estimation due to current measurement.

Thesis Supervisor: Pablo Garcia

Title: Associate Professor

Thesis Supervisor: Igor Cantero

Title:

Acknowledgments

I would like to thank professor Pablo Garcia for his advice and encouragement throughout this thesis, and Fernando Perez for his support during the experimental testes of my work. I would like also to thank Dr. Igor Cantero and the rest of Cegasa Portable Energy R&D teams for their kind treatment.

Table of Contents

Chapter 4

Chapter 5

Chapter 1

Introduction

This is an introduction chapter of lithium ion battery cell modelling. In this first chapter, the motivations for modelling of lithium ion battery are discussed and related literatures are reviewed. Objectives and scope of the work are presented.

1.1 Motivation

Emission and geopolitical concerns of fossil fuel dependency are pushing the globe to look for alternative sources for energy production and transportation. Introducing large amount of renewable towards the energy sector and electrifying the transportation sector beside using optimized and energy saving technologies are the main strategies being realized as a solution for such issues. This has opened a new era for battery storage systems as a key technology in those sectors. The market is working towards developing high energy and power density storage systems to meet the demand. Considering the transportation sector, electric vehicle (EV) and hybrid electric vehicles (HEV) are now gaining popularity once again. However, the success of the technology depends on the advancement of the storage system deployed in terms of efficiency, stability, energy density and recharging speed. This is because of EV and HEV are needed to have longer driving rage and shorter refilling time. Since the last decade, with safety improvement and affordable price, lithium ion batteries have become attractive in EV and HEV application over nickel cadmium and nickel metal hydride batteries. High specific energy, long lifetime and low self-discharge compared to other storage systems make them preferable. Large scale lithium batteries are also being introduced in the energy sector to improve the grid flexibility and support the renewable energy sources.

Lithium ion batteries have sensitive operating ranges in terms of voltage and temperature. Performance and safety are the main considerations in the design and battery operation process. Knowing the behavior of the battery and monitoring it while running help to improve the efficiency and lifetime. Battery management in real-time and performance analysis techniques play a key role in this regard. System modeling plays vital for analyzing and predicting of battery behavior. Battery storages are highly non-linear electrochemical systems and their performance isn't like ideal energy

sources. It is governed by complex mixture of laws of thermodynamics, electrode kinetics, ion transport and diffusion phenomena. By designing a model which considers internal and external conditions of the system, the battery behavior can be predicted or simulated. Two approaches of modelling are common in electrochemical battery storage systems. The first one is, deriving the electrical and thermal property from physical laws which govern electrochemical reaction inside the cell. It is known as Electrochemical Model (ECM) or physics based model. This approach is more accurate, however the nonlinear partial differential equations involved in the physical laws and having coupled parameters make the approach computationally more intensive and sometimes difficult to solve the equations. The other approach is Electrical Equivalent Circuit (EEC) based modelling technique, electrochemical behavior of the battery is represented using active and passive electrical elements. A voltage source connected in series with a resistor is widely used battery model, where the voltage source represents open circuit voltage and the resistor to model the internal impedance. Such simple models don't satisfy accuracy requirement in all applications and usually one or more parallel resistor-capacitor networks are included to capture the dynamics better. EEC battery models require characterization tests which may need expensive laboratory equipment for parameter estimation.

The purpose of modelling can vary based on the issue being addressed. Battery Management System (BMS), Load performance analysis and Battery design process are the main application areas.

> *BMS*: It is an electronic system with software algorithms to manage the operation of the battery and protect the battery from working in undesirable conditions. BMS can be simple or sophisticated that also performs secondary operations to satisfy the application requirements. Compared to other type of batteries, Lithium ion batteries are not voltage tolerant. For safe battery operation and extended life, an algorithm which estimates the state of charge (SOC) and state of health (SOH) of the battery from voltage-current measurement is essential. Estimation algorithms are based on the battery model. The type of modelling and parameter estimation algorithms implemented determines the computational requirements and accuracy of the BMS which influences the final cost of the battery. Simplified ECM and EEC Models are popular in BMS.

Load Performance Analysis: In this regard modelling is required to simulate load characteristics under different operating condition either in cell or battery pack level. For instance, in ''hardware in the loop'' analysis which incorporate the battery as a system level component, the battery behavior should be modelled and implemented. Simulation model is also needed to analyze the performance of the battery in hybrid power systems.

Battery Design: Modelling is crucial in studying electrochemical process inside the battery cell either to design application specific battery cells or improve the performance of the battery. Underutilization, capacity fade up and thermal runway are some of the issues which should be considered during battery design. Multiphysics modelling approach is common in battery design process.

1.2 Literature Review

To improve the performance of lithium ion batteries in varies applications, EEC based modelling are proposed and used for state of charge estimation. Coulomb counting is the simplest to estimate and implement. The technique suffers from accumulation error due to current measurement. Voltage based SOC estimation is also applicable in some type of batteries. It is not a good option for lithium ion batteries because of Open Circuit Voltage (OCV) curve is flat in certain rage of SOC which makes the technique ineffective. Model based SOC estimation is the most effective technique in battery BMS and system performance analysis. Commonly a resister and single parallel resistor-capacitor is considered as the cell impedance. Those type of models are good enough to capture the performance of the battery and simplify parameter estimation process. Researchers are looking for better parameter estimation techniques. Kalman based filters, and other novel adaptive methods are the most discussed SOC estimation techniques with model based methods [1] [2] [3] [4]. In [5] Neural Network based model is discussed with Unscented Kalman Filter to reduce the error in the model. Beside SOC estimations, lithium ion battery model is also used in predicting thermal behavior. In most BMS, lumped parameter thermal modelling approach is preferred due to its simplicity. Heat is generated inside the battery cell from two source, electrochemical reaction and joule loss and the energy balance equation comes from the entropy change and heating due to joule loss. Novel parametric circuit modelling for lithium ion battery which is applied for performance simulation and thermal analysis of electric vehicles is discussed in [6]. Non-negative least square with genetic algorithm is applied to estimate model parameters to avoid the estimated parameters being negative. The model parametrization is done for three parallel

Resister-Capacitor (RC) EEC model. In [7] and [8] Simulink model of lithium ion battery for hybrid power system testbed is proposed. Both [6] and [7] considered only the effect of SOC while estimating impedance parameters, however [8] considered also current effect. A battery pack integrated equivalent circuit and thermal model for temperature dependent embedded applications is proposed in [9]. A single RC based EEC is used to model electrical and thermal behavior of 12 cell battery pack from 5-45°C. The model parameters are both estimated and validated only using pulse discharge test which do not guarantee dynamic robustness of the model.

In this thesis EEC based Simulink/Simscap model is proposed. The model considers the variation of impedance parameters with SOC, temperature and current. The model also consists of three RC branches considering the future extension of the work to include the degradation effect of the battery cell in the model. The parameters are estimated from modified Hybrid Pulse Power Characterization (HPPC) test and the model is validated with Dynamic Stress Test (DST), and pulse discharge tests beside HPPC which assured the robustness of the model.

1.3 Objective

The general objective of this work is developing a lithium ion battery model which simulates the performance of the battery in terms of electrical, and temperature effect. It consists the following specific objectives:

1. Review literature regarding lithium ion battery technology and modelling techniques.
2. Propose an equivalent electric circuit model for electrical and thermal simulation of the battery cell.
3. Perform static capacity and dynamic experimental tests to collect data for the battery cell parameter estimation and model validation.
4. Estimate the battery cell parameters at different working conditions (i.e. SOC, temperature).
5. Prepare temperature dependant battery cell MATLAB model using Simulink and Simscape tool boxes.
6. Validate the model at different operating conditions.

1.4 Scope of the Thesis

This thesis is the first part of developing a full MATLAB simulation package for electrical, thermal and degradation behavior of lithium ion battery. The scope of the thesis is developing simulation

model for the electrical behavior of the battery cell from 10 ℃ to 40℃ temperature and up to 3C discharge current from 0 to 100% state of charge conditions. The model also considers connecting the cells in parallel or series for further battery pack level simulation.

1.5 Thesis Outline

The remaining of this paper is presented as the following. Chapter two explains the state of the art for the thesis. In this chapter, the application of energy storage system and various storage technologies are discussed. Lithium ion battery cell modelling approaches, electrochemistry and electric equivalent circuit based, are presented. Parameter estimation techniques for EEC model are also explained in this chapter. The methodology of the thesis is in chapter three, which states about the proposed model, experimental setups for data measurement and analysis and parameter estimation of the model. The MATLAB based simulation model is developed in the fourth chapter, which shows Simulink and Simscape techniques for modelling the open circuit voltage, state of charge estimation and lamped RC parameters of the cell. In Chapter five simulation results are discussed and the model is validated. Conclusion and future works are presented in chapter six. Finally, Chapter seven and eight contains the bibliography and appendices of the work respectively.

Chapter 2

State of The Art

This is the chapter where previous knowledges and development techniques of the problem, which is lithium ion battery cell modelling, are presented. It starts from ESS definition and Types of ESS regarding the energy form stored. Basic characteristics and performance of each storage systems are also stated. Various lithium ion battery technologies are presented and compared. Numerical and empirical modelling approaches for lithium ion battery cell are reviewed. Two data measurement techniques i.e. frequency and time domain techniques for empirical modelling are discussed. Various SOC estimation techniques with pros and cons are also presented.

2.1 Energy Storage Systems (ESS)

Due to basic characteristic of electricity to be consumed at the time it is generated, there is a need to store electrical energy for use on demand. The energy cannot be stored directly, however it can be stored in other forms of energy and converted back to electricity. This brings the need for an energy storage technology or a device which stores the electrical energy in other forms such as chemical, potential, kinetic and thermal. EES is a key technology in utilizing world's energy resources effectively. It brings flexibility in providing energy at the choice of time. Nowadays there is an emerging need for ESS in grid, transportation applications and portable devices. Reduction of emission and being independent from fossil fuels, a need for sustainable energy source, and make the existing grid smarter are the main driving forces towards the technology.

2.1.1 ESS Types

ESSs varies in terms of their functions, response time, and suitability for the application. The most common classification method is based on the form of energy stored in the system [10] [11]. Figure 2-1 summarizes the classification of ESS based on the energy form. Including the technology maturity and cost, choice of specific type of storage system for an application depends on the maximum energy and power rating needed, required response time during charge-discharge, system weight and volume constraints, and suitable operation temperature. Figure 2-2 describes comparison of various energy storage technologies regarding their energy and power capacity. Not all storage systems fulfill both energy and power requirements. Supercapacitors and super conducting coils have good response time and can deliver high power output. However, their

energy storage capacity is low. In contrast pumped hydro and flow batteries can store large amount of energy but their response time is lower. Most of the time characteristics of the application selects which ESS is suitable.
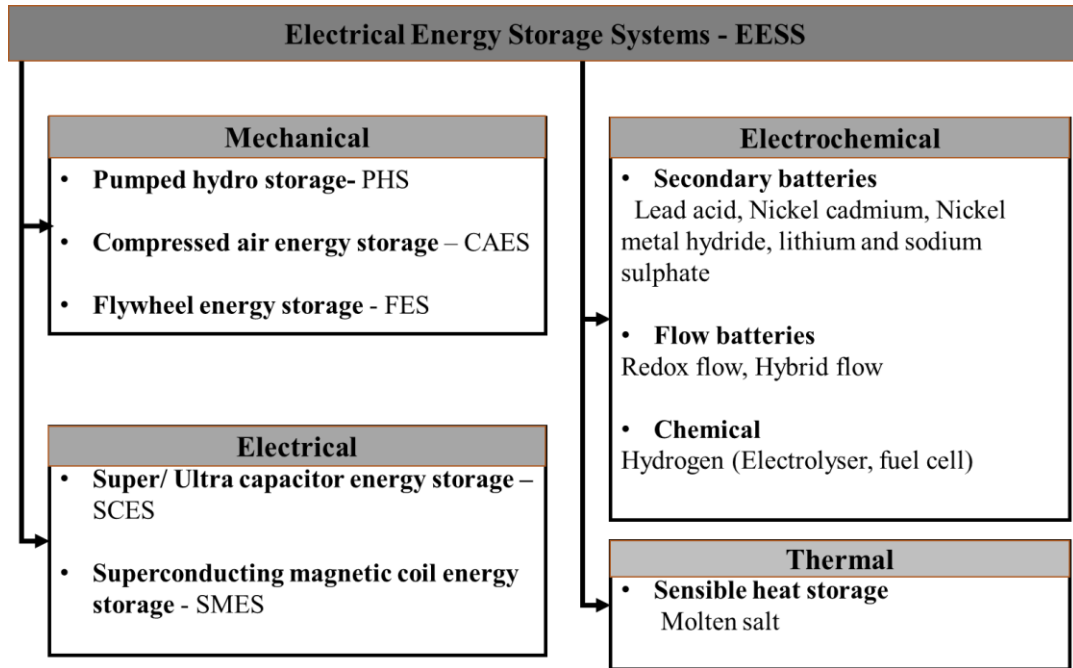

Figure 2-1 Classification of ESS based on the energy form

The role of ESS in power sector can be seen in different stages from generation to utility and consumer level. In generation stations, it is being used as time shifting by storing the surplus power when it is not needed and to increase supply capacity. It also helps as a frequency control function to improve power quality. Pumped Hydro Storage (PHS), Compressed Air Energy Storage (CAES), traditional electrochemical batteries, flow batteries and hydrogen are among the technologies in generation plants. In utilities, it may play as a cost saving method for storing energy during off peak hour with less price beside keeping power quality, efficient use of the power network and supplying power during emergency to maintain service reliability. Traditional electrochemical batteries, Superconducting Magnetic Energy Storage (SMES), Super capacitors are used in addition to flow batteries and CAES. Consumers may also use ESS for saving cost by time shifting the energy due to time varying price of the electricity. It can be also considered as emergency power source in power sensitive applications during power outage instead of power generators. Lithium

ion, lead acid, flywheel and flow batteries are preferable energy storage technologies. The other potential application of ESS is renewable energy generation sectors.
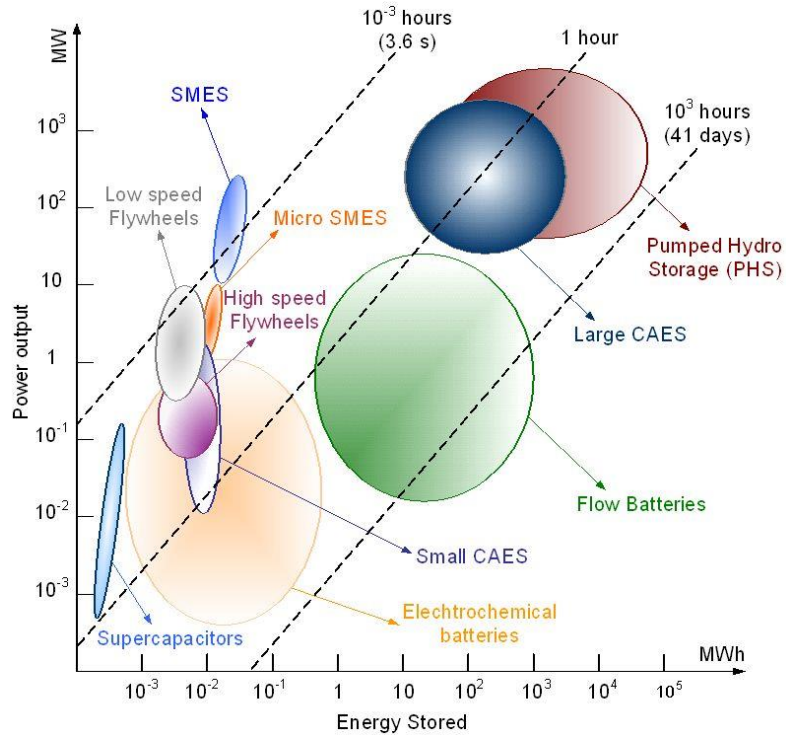

Figure 2-2 Comparisons of energy storage technologies [12]

Utilizing more renewable energies in the power system grid reduces the emission and fossil fuel dependency issues. However, the energy from renewable sources such as wind and solar, is unreliable and causes power fluctuation issue. This makes the system unable to maintain output and meet power demand. By introducing ESS in power systems, more efficient use of renewable energy can be realized, the issue of intermittency during grid integration of renewables is also addressed by delivering energy only when the grid needs.

Transportation sector is one of the greatest contributor of greenhouse gas emission. In Europe transportation sector accounts 23% from the total greenhouse gas emission based on 2015 statics [13]. In the same year, in United state transportation represented 27% of the total emission in the country [14]. Electrification of the transportation sector, such as electrified railways, electric and hybrid vehicles powered by electricity, is becoming a promising alternative to alleviate dependency of fossil fuel and improve urban life. Unlike grid and energy sector applications, electric/hybrid

8

electric vehicles desire high energy and power density storage systems. Driving range and charging time are important factors for success of electric vehicles. High performance batteries are needed to be mounted in Electric vehicles as a power source. The technology is also being improved to use vehicle storages to power home appliances and support the grid by connecting them in the time of need which is known as vehicle to grid application [15]. Battery storage system particularly Lithium ion and NMH are the widely used batteries in electricity powered vehicles [16].

2.1.2   **Battery Storage Systems (BSS)**

Battery storage systems are electrochemical systems which includes primary, secondary and flow batteries. Lead acid, nickel and lithium ion are widely used secondary batteries for both stationary and non-stationary applications. Secondary batteries are rechargeable batteries which have cells with reversible chemical reaction on charge and discharge. Anode, cathode and separator are the main components of a battery cell. Based on the required nominal voltage and capacity, the battery cells are connected in series and parallel. Figure 2-3 summarizes typical cell voltage and chemical reaction on anode and cathode during charge-discharge of various rechargeable batteries.

Components of a Battery Cell

Anode: It is an electrode which releases electrons during discharge and accepts electron on charge. It is negative on discharge and positive on charge. Efficiency, specific capacity and conductivity are important parameters to select anode material. Stability, manufacturing simplicity and cost are also decisive factors.

Cathode: It is an electrode which absorbs electron during discharge and release on charge. It is positive on charge and negative on discharge. Cathode material is selected based on its voltage and chemical stability.

Separator: it is a material which isolates the anode and electrode electrically. It allows the movement of ions from one electrode to the other. Electrical insulation, minimum ionic resistance, mechanical stability and prevention of particles migration are some of the required parameters for separator materials.

Electrolyte: A nonmetallic substance placed between anode and cathode electrodes. It promotes movement of ion between cathode and anode which makes the battery conductive. The electrolyte

of a battery consists of soluble salts, acids or other bases in liquid, gelled and dry formats. It can be also a polymer form, like in solid-state batteries, solid ceramic and molten salts, as in the sodium-sulfur battery. The electrolyte should be highly conductive, non-reactive with the electrode materials and stable with operating conditions such as temperature.

Secondary batteries store and release electrical energy up to a certain number of cycles. The maximum number of cycle and other performance characteristics of batteries vary based on the chemistry and material in it.

Rechargeable Batteries

Lead acid battery: exploring lead-acid battery as energy storage device dates back 1800s [11]. It is the most widely used rechargeable electrochemical storage system. It has lead dioxide (Pbo_2) cathode and sponge lead (Pb) anode, with sulfuric acid electrolyte. Lead acid batteries has fast response time, small daily self-discharge rate and relatively high cycle efficiency. Its cost is also low and has high reliability. It has been developed as a power source for hybrid and electric vehicle, however its application in utility is limited due to low number of cycles.

Lithium ion battery: Lithium ion battery has a cathode made up of lithium metal oxide (such as $LiCoO_2$, $LiFePO_4$ and $LiMO_2$) and the anode is typically graphite carbon. The electrolyte consists of lithium salts dissolved in organic carbonates. During charging process, the lithium-ions travel from cathode to anode. Then lithium ions combine with external electrons and are deposited between the carbon layers as lithium atoms. The process reverses during discharge. Lithium ion batteries have good energy to weight ratio, no memory effect, and low self-discharge. They are good candidate for applications need fast response time and have dimension and weight constraint. The protection circuit and battery management system makes lithium ion batteries more expensive than other chemical batteries.

Nickel Cadmium (NiCd): Nickel-cadmium battery contains a nickel hydroxide as positive electrode and cadmium hydroxide as negative electrode. It has an alkaline electrolyte. NiCd battery is robust and has high reliability and low maintenance cost. The downsides of NiCd battery are: cadmium is toxic, resulting in environmental hazards, the battery suffers from the memory effect

which means, the maximum capacity can be dramatically decreased when the battery is repeatedly recharged after being only partially discharged.

Nickel Metal Hydride (NMH): NMH battery is like NiCd except hydrogen is used as electrode instead of cadmium. It has moderate specific energy and relatively high energy density which makes the battery better than NiCd. It has also reduced memory effect and is environmentally friendly. It is used from portable device up to hybrid and electric vehicles and standby industrial applications. However, it has high rate of self-discharge. The performance also decreases after a few hundred full cycles.

Sodium Sulphur/ Sodium Nickel Chloride: unlike other battery technologies, sodium-nickel-chloride (zebra batteries) and Sodium-Sulphur batteries have a solid-state electrolyte. Sodium Sulphur battery consists of liquid Sulphur at anode electrode and liquid sodium at cathode electrode. The positive sodium ions are pass through the electrolyte and combines with Sulphur to form a sodium poly-sulphide. The zebra battery has moderate specific energy, energy density, specific power, and a high operating temperature.

Battery type	Chemical reactions at anodes and cathodes	Unit voltage
Lead–acid	$Pb + SO_4^{2-} \Longleftrightarrow PbSO_4 + 2e^-$	2.0 V
	$PbO_2 + SO_4^{2-} + 4H^+ + 2e^- \Longleftrightarrow PbSO_4 + 2H_2O$	
Lithium-ion	$C + nLi^+ + ne^- \Longleftrightarrow Li_nC$	3.7 V
	$LiXXO_2 \Longleftrightarrow Li_{1-n}XXO_2 + nLi^+ + ne^-$	
Sodium–sulfur	$2Na \Longleftrightarrow 2Na^+ + 2e^-$	~2.08 V
	$\chi S + 2e^- \Longleftrightarrow \chi S^{2-}$	
Nickel–cadmium	$Cd + 2OH^- \Longleftrightarrow Cd(OH)_2 + 2e^-$	1.0–
	$2NiOOH + 2H_2O + 2e^- \Longleftrightarrow 2Ni(OH)_2 + 2OH^-$	1.3 V
Nickel–metal hydride	$H_2O + e^- \Longleftrightarrow 1/2H_2 + OH^-$	1.0–
	$Ni(OH)_2 + OH^- \Longleftrightarrow NiOOH + H_2O + e^-$	1.3 V
Sodium nickel chloride	$2Na \Longleftrightarrow 2Na^+ + 2e^-$	~2.58 V
	$NiCl_2 + 2e^- \Longleftrightarrow Ni + 2Cl^-$	

Figure 2-3 Anode-Cathode chemical reactions and cell voltages of battery technologies [10]

Some characteristics and performance of the above battery technologies are presented and compared in Figure 2-4. The figures in the table are based on average ratings of commercial batteries and special batteries with above average ratings are excluded. Lithium ion batteries have higher cell voltage and low toxicity. They have also a peak current of more than 30C. As shown in

the figure lead acid batteries have cycle life only from 200 to 300. Lithium batteries go up to 2000 cycles for 80% discharge.

Specifications	Lead-Acid	NiCd	NiMH	Li-Ion		
				Cobalt	Manganese	Phosphate
Specific energy density (Wh/kg)	30 – 50	45 – 80	60 – 120	150 – 190	100 – 135	90 – 120
Internal resistance (mΩ/V)	<8.3	17 – 33	33 – 50	21 – 42	6.6 – 20	7.6 – 15.0
Cycle life (80% discharge)	200 – 300	1,000	300 – 500	500 – 1,000	500 – 1,000	1,000 – 2,000
Fast-charge time (hrs.)	8 – 16	1 typical	2 – 4	2 – 4	1 or less	1 or less
Overcharge tolerance	High	Moderate	Low	Low	Low	Low
Self-discharge/month (room temp.)	5 – 15%	20%	30%	<5%	<5%	<5%
Cell voltage	2.0	1.2	1.2	3.6	3.8	3.3
Charge cutoff voltage (V/cell)	2.40 (2.25 float)	Full charge indicated by voltage signature	Full charge indicated by voltage signature	4.2	4.2	3.6
Discharge cutoff volts (V/cell, 1C*)	1.75	1	1	2.5 – 3.0	2.5 – 3.0	2.8
Peak load current**	5C	20C	5C	> 3C	> 30C	> 30C
Peak load current* (best result)	0.2C	1C	0.5C	<1C	< 10C	< 10C
Charge temperature	-20 – 50°C	0 – 45°C	0 – 45°C	0 – 45°C	0 – 45°C	0 – 45°C
Discharge temperature	-20 – 50°C	-20 – 65°C	-20 – 65°C	-20 – 60°C	-20 – 60°C	-20 – 60°C
Maintenance requirement	3 – 6 months (equalization)	30 – 60 days (discharge)	60 – 90 days (discharge)	None	None	None
Safety requirements	Thermally stable	Thermally stable, fuses common		Protection circuit mandatory		
Time durability				>10 years	>10 years	>10 years
In use since	1881	1950	1990	1991	1996	1999
Toxicity	High	High	Low	Low	Low	Low

*Peak load current - Maximum possible momentary discharge current, which could permanently damage a battery

*'C' refers to the battery capacity

Figure 2-4 Characteristics of commonly used rechargeable batteries [17]

Battery Terminologies

C-rate: It is a measure of the rate at which a battery is discharged relative to its maximum capacity. A 1C rate means the discharge current will discharge the entire battery in 1 hour. For instance, for a battery with a capacity of 100 Amp-hrs, this equates to a discharge current of 100 Amps.

SOC: An expression of the present battery capacity as a percentage of maximum capacity.

Depth of discharge (DOD): The percentage of battery capacity that has been discharged expressed as a percentage of maximum capacity.

Nominal capacity: The energy capacity of the battery, the total Watt-hours available when the battery is discharged at a certain discharge current from 100 percent state-of-charge to the cut-off voltage.

Nominal voltage: The reported or reference voltage of the battery by the manufacturer, which is considered as the "normal" voltage of the battery.

Cut-off Voltage: The minimum allowable voltage. It is this voltage that generally defines the "empty" state of the battery.

2.1.3 Electrical Storages

Electrical storages include supercapacitors and super conducting coils which store energy in the form of electric charges.

Super capacitors (Ultra capacitors): Supercapacitors consists of two electrodes, electrolyte and a membrane in which ions can travel. The amount of energy stored depends on the surface area of the electrode and the distance between them. The basic difference between super capacitors and ordinary capacitors is, super capacitors use porous electrodes which increase the surface area of the electrodes. Super capacitors may be double layer capacitors where charge storage is electrostatically or pseudo capacitors where the charge storage is electrochemical. Hybrid types are also available.
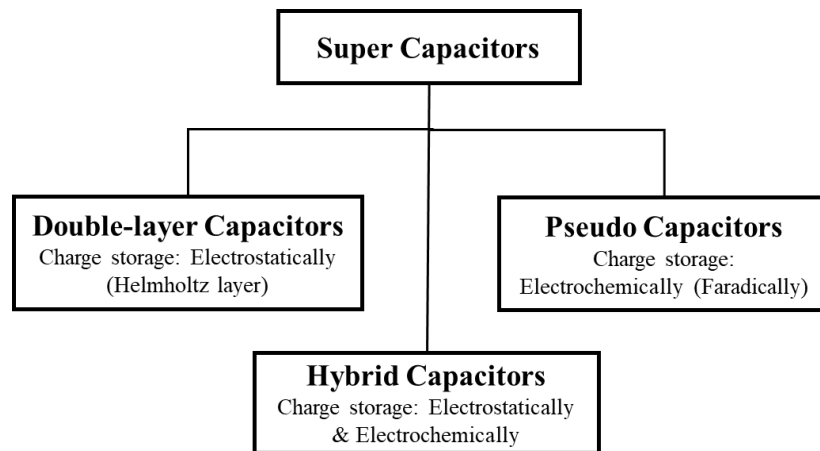
Figure 2-5 Super capacitors based on charge storage

SMES: stores energy using super conducting coil in the form of magnetic field. It consists of two parts, cryogenically cooled superconducting coil and power conditioning system. The magnetic field is created with the flow of a direct current (DC) through the coil. To maintain the system charged, the coil must be cooled adequately. This enables the current to circulate indefinitely with almost zero loss, and therefore, the energy remains stored in the form of a magnetic field. The stored energy can be released back to a connected power system by converting the magnetic energy to electricity, which is discharging the coil. The only conversion process in superconductors is from AC to DC in the power conversion stage so it has high cycle efficiencies. This very high cycling capacity and efficiency over short time periods make SMES very well suited to high power short duration applications. SEMS also has the ability of fast response, however the main drawback is it need large amount of power to keep the coil at low temperature.
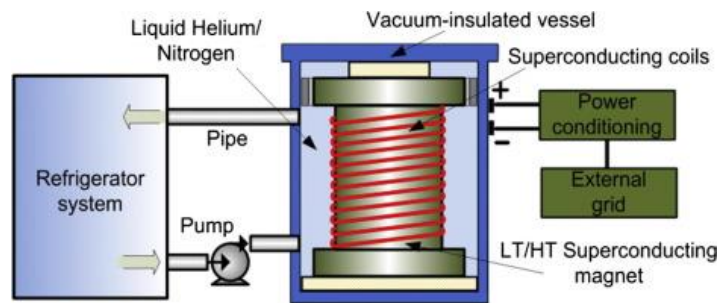
Figure 2-6 Typical illustration of SEMS system [18]

2.1.1 Hybrid Battery Supercapacitor Storage Systems (HBSSS)

HBSSS contains electrochemical battery for long term storage and supercapacitor to support fast dynamics. It is shown that battery storages cannot satisfy both energy and power requirements of all applications. Batteries in general are good to store large amount of energy, however they are slow in transferring the energy. In contrast Supercapacitors or Super conductor coils are fast in transferring the stored energy, effective in supporting short term peak currents. In applications which are sensitive for both energy and power, such as renewable energies, electric vehicle and others, both requirements can be satisfied by HBSSS. Researches are being done to optimize such hybridization and to analyze the economic benefits [19], [20]. In [21] the hybrid battery supercapacitor storage system is critically reviewed and compared with the well-established battery storages (lead acid, nickel metal hydride lithium ion, …) in terms of power quality, system complexity, life span and system cost based on renewable and electric vehicle applications. The

basic challenge in the hybridization is the extra cost and system reliability due to the controller electronics needed. However, the controller and management electronic is also available even in some battery storage systems, such as lithium ion battery, to secure safety and stability.

2.1.2   **Lithium Ion Battery Technologies**

Lithium ion batteries are of the most popular energy storage technology since last decade due to capability of having high energy density, high power density, high efficiency, low self-discharge rate and long lifetime. Lithium ion battery doesn't specify a single chemistry reaction, rather it specifies a battery which has an insertion reaction both on the cathode and anode in which a lithium ion acts as a charge carrier, though at the beginning it was defined only for batteries which utilizes intercalation reaction [22]. Some chemistries are popular with their special characteristics and performances: Lithium cobalt oxide-LCO ($LiCoO_2$ cathode) which has high specific energy with low thermal stability, life time and specific energy; Lithium manganese oxide- LMO ($LiMn_2O_4$ cathode) or blended lithium nickel manganese cobalt oxide-NMC ($LiNiMnCoO_2$) to improve specific energy and life span; Lithium iron phosphate-LFP ($LiFePO_4$ cathode) which has good safety characteristics; Lithium titanium oxide-LTO ($Li_4Ti_5O_{12}$ as $negative$ $electrode$) which has long life and good safety. Table 2-1 summarizes common cathode chemistries and their application areas including the abbreviations which they are known in research papers and manufacturer datasheets.

Table 2-1 Lithium ion battery technologies [23]

Chemical Name	Material	Abbreviation	Applications
Lithium cobalt oxide	$LiCoO_2$	LCO	Cell phones, laptops, cameras
Lithium manganese oxide	$LiMn_2O_4$	LMO	Power tools, EVs, medical, hobbyist
Lithium iron phosphate	$LiFePO_4$	LFP	Power tools, EVs, medical, hobbyist
Lithium nickel manganese cobalt oxide	$LiNiMnCo0_2$	NMC	Power tools, EVs, medical, hobbyist
Lithium nickel cobalt aluminum oxide	$LiNiCoAlO_2$	NCA	EVs, grid storage
Lithium titanate	$Li_4Ti_5O_{12}$	LTO	EVs, grid storage
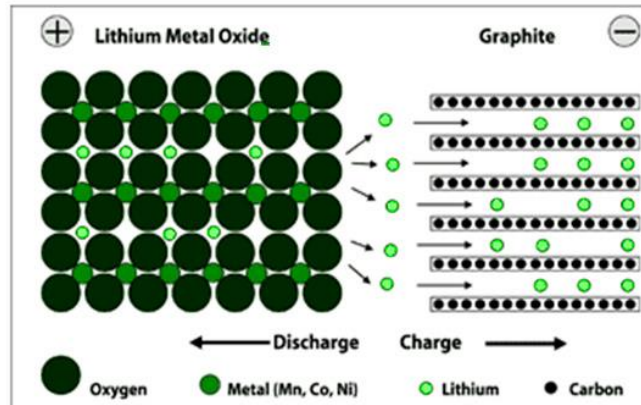
Figure 2-7 lithium ion battery cell demonstration on charge and discharge [17]

Figure 2-8 compares different lithium ion battery technologies about the basic application characteristics. The size of extension of the denser color indicates the technology good in that dimension.
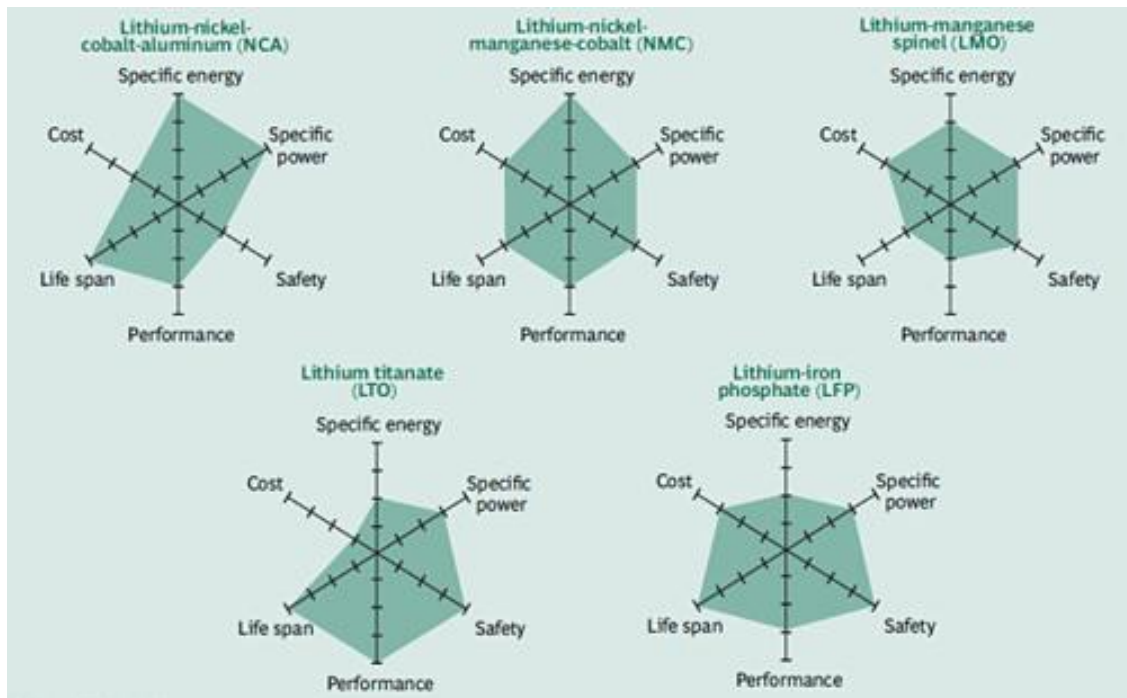
Figure 2-8 Comparison of lithium ion battery technologies [23]

2.2 Electrical Modelling of Lithium Ion Cell

The electrochemical and thermal behavior of lithium ion cells vary under different operating conditions. Lithium battery cells are voltage sensitive, cells should operate under specified voltage limits and temperature ranges. For better battery management and performance analysis, having a model with high accuracy is important. Two approaches of modelling are used in literature: Electrochemical (physics based) and Equivalent Electric Circuit (empirical based) model. Various modelling approaches are also under each category which differs in their level of details. The choice of a battery model type requires a trade-off in model complexity and accuracy. In some literature mathematics based artificial intelligent techniques like Neural Network are also proposed.

2.2.1 Electrochemical Models (ECMs)

In this approach, the system model is derived from non-equilibrium thermodynamics transport and reaction equations based on concentrated solution theory. The electrochemical dynamics of the battery is represented by partial differential equations which represents the physical phenomena inside the cell during charging/discharging. ECMs are very helpful to analyze the effect of physical properties and particle distributions in the battery performance. Charge transfer, circuit potential, diffusion, and double layer effect are the main physical phenomena for electrothermal characterization of a battery cell. Doyle, Fuller and Newman originally developed Pseudo 2 Dimensional (P2D) electrochemical dynamic model for a single material electrode [24]. However due to the computational burden and difficulty in solving system's partial differential equations, it is not easy to apply the model in advanced control and management systems. Since then different approximation and assumptions are considered to reduce structural complexity and simplify parameter identification process. Pade and Parabolic approximations [25] are some of the techniques used by researchers to achieve confined and physically meaningful electrochemical model. ECM approach is based on Butler-Volmer equation, Porous electrode theory, concentrated solution theory and potential drop in the solid conducting phase which is described by ohms' law. Porous electrode theory is the earliest for mathematical framework of non-equilibrium thermodynamics of porous electrode [26]. It is based on Butler-Volmer reaction kinetics equation, shown in equation 2-1, which describes the Faradaic current density. The equation explains the relation of current on each electrode with the electrode potential and reaction kinetics. It defines the electrochemical dynamics on the electrodes surface. Researchers are also proposed a modified

porous electrode theory using modified Butler-Volmer equation and classic porous electrode equations to find thermodynamically consistent equation for their model.

$$j = j_0 \cdot \left\{ e^{\frac{\alpha_a zF}{RT}(\phi_s - \phi_e - U_{oc})} - e^{-\frac{\alpha_c zF}{RT}(\phi_s - \phi_e - U_{oc})} \right\} \tag{2-1}$$

$$j_0 = K(C_e)^{\alpha_a}(C_{s,max} - C_{s,surf})(C_{s,surf})^{\alpha_c} \tag{2-2}$$

Where, j is electrode current density (A/m^2), j_0 exchange current density (A/m^2), E electrode potential (V), E_{eq} equilibrium potential (V), K absolute temperature (K), z number of electrons involved in the reaction, F Faraday's constant, R universal gas constant, α charge transfer coefficient (anode and cathode),

C_e concentration in electrolyte, C_s concentration in solid phase, and η activation overpotential.

$$\eta = \phi_s - \phi_s - U_{oc} \tag{2-3}$$

The exchange current density, j_0 depends on the lithium ion concentration in the electrode and electrolyte. This value can be approximated as a constant if the battery is excited with low amplitude current during electrochemical impedance spectroscope analysis [27].

The open circuit potential of the anode and cathode can be derived from Nernst equation as shown in below. It can be also approximated by linear functions or higher order polynomials to fit the property.

$$E_{cell} = E_{cell}^o - \frac{RT}{zF} ln Q_r \tag{2-4}$$

Where, E_{cell} is the cell potential, E_{cell}^o standard cell potential, Q_r is reaction quotient.

Species conservation of lithium ion and charge both in electrolyte and solid phase including the initial and boundary conditions are also governing relations in electrochemical based modelling. The schematic of one-dimensional (pseudo 2 dimensional-P2D) model is shown in Figure 2-9 which comprises porous negative and positive electrode, separator and electrolyte. While the battery is discharging, lithium ions diffuse to the surface of the electrode to make electrochemical reaction and join the electrolyte, then the ions travel to the other side of the solid electrode via

18

diffusion and migration by crossing the separator and intercalate themselves. P2D is successful electrochemical model to describe the conservation of mass and charge both in solid and electrolyte phase which is based on fixed particle radius [28]. Concentration of lithium ions also affected by the diffusion inside the active materials (anode and cathode). This diffusion behavior in electrodes is explained by Fick's second law which is stated in equation 2-6 and 2-7 for mass (lithium ions) conservation in the solid and electrolyte phase.

$$\frac{\partial C_s(x,r,t)}{\partial t} = \frac{D_s}{r^2}\frac{\partial}{\partial r}\left(r^2\frac{\partial C_s(x,r,t)}{\partial r}\right)$$
(2-5)

Boundary conditions:

$$\frac{\partial C_s}{\partial t}\Big|_{r=0} = 0, D_s\frac{\partial C_s}{\partial t}\Big|_{r=Rs} = \frac{-j}{aF}$$
(2-6)

Where, C_s is the concentration in solid phase, D_s diffusion coefficient, x is the dimension of the cell as shown in figure 1, r radius of the spherical particle, j rate of electrochemical reaction in the solid phase, and t is time.

Conservation of lithium ion in the electrolyte phase is also stated as:

Negative and positive electrode;

$$\varepsilon_e\frac{\partial C_e}{\partial t} = \frac{\partial}{\partial t}\left(D_e^{eff}\frac{\partial C_e}{\partial x}\right) + \frac{1-t_+^0}{F}j$$
(2-7)

Separator;

$$\varepsilon_e\frac{\partial C_e}{\partial t} = \frac{\partial}{\partial t}\left(D_e^{eff}\frac{\partial C_e}{\partial x}\right)$$
(2-8)

Boundary conditions:

Current collector interface:

$$\frac{\partial C_e}{\partial t}\Big|_{x=0} = 0, \frac{\partial C_e}{\partial t}\Big|_{x=L_{cc}} = 0$$
(2-9)

Negative electrode separator interface:

19

$$C_e|_{x=L_n^+} = C_e|_{x=L_n^-} \qquad (2\text{-}10)$$

$$D_e^{eff} \frac{\partial C_e}{\partial t}|_{L_n^+} = D_e^{eff} \frac{\partial C_e}{\partial t}|_{L_n^-} \qquad (2\text{-}11)$$

Positive electrode separator interface:

$$C_e|_{x=L_p^+} = C_e|_{x=L_p^-} \qquad (2\text{-}12)$$

$$D_e^{eff} \frac{\partial C_e}{\partial t}|_{L_p^+} = D_e^{eff} \frac{\partial C_e}{\partial t}|_{L_p^-} \qquad (2\text{-}13)$$

Charge conservation in the solid phase (electrodes) is described using ohm's law:

$$\frac{\partial}{\partial x}\left(\sigma^{eff} \frac{\partial}{\partial x} \phi_s(x,t)\right) - j(x,t) \qquad (2\text{-}14)$$

With boundary conditions:

$$-\sigma^{eff} \frac{\partial \phi_s}{\partial x}|_{x=0} = +\sigma^{eff} \frac{\partial \phi_s}{\partial x}|_{x=L_{cc}} = \frac{I}{A} \qquad (2\text{-}15)$$

$$\frac{\partial \phi_s}{\partial x}|_{x=L_n} = \frac{\partial \phi_s}{\partial x}|_{x=L_n+L_s} \qquad (2\text{-}16)$$

Where, ϕ_s is the potential of electrode, σ^{eff} is effective electrode conductivity.

Parameters in the above equations are either experimentally determined or estimated. Finding analytical solutions for the above coupled partial differential equations is complicated because of electrochemical parameter variation in each domain and necessity of spatial discretization to convert PDE to Ordinary Differential Equations (ODE) [29]. Using numerical methods, the PDEs can be reduced in to ODEs and then to algebraic differential equations for solving the above system equations [25]. The detail electrochemical model could have more than six state variables [30] [31], including the solid electrode potential, electrolyte potential, anode and cathode lithium ion concentration, lithium ion concentration in the electrolyte, ionic current in the electrolyte and Faradaic current density between active material in the electrode and electrolyte.
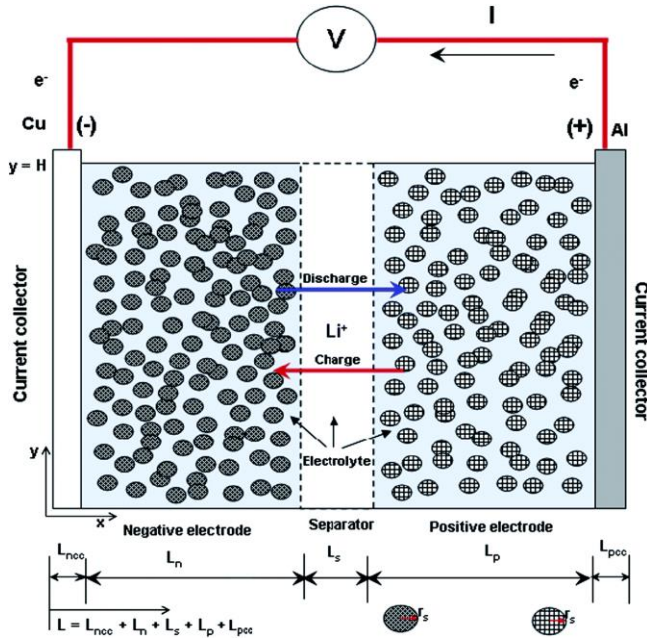
LFP Cell Reactions

$$Li_x C_6 \rightarrow C_6 + xLi^+ + xe^-$$
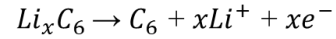
(reaction in the negative

electrode during discharge)

$$Li_{1-x} F_e PO_4 + xLi^+ + xe^- \rightarrow LiF_e PO_4$$
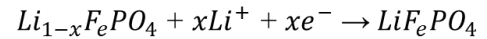
(reaction in the positive

electrode during discharge)

Figure 2-9 Schematic of the lithium ion battery electrochemical model and discharge reaction equation for LFP [6].

However, models with high computational efficiency while maintaining acceptable precision is realistic. In literature, several works are proposed to reduce electrochemical models. Those researches are mainly focused on either on reducing computational complexity of solving lithium ion concentration in solid electrode particle or reducing the complexity of the electrochemical model. Single Particle Model (SPM) which has one partial differential equation and an algebraic equation is most practical [31]. SPM assumes the current to the battery is small and the electrolyte has large conductivity. In [30] simpler electrochemical model based on SPM with two differential algebraic equations and one algebraic equation is also proposed, in which the lithium ion concentration in the electrodes is represented by a polynomial function with respect to the particle radius. A transfer function type of simplified electrochemical model is also proposed in [29] which is based on modified boundary conditions and Pade approximation technique of the electrolyte diffusion equation. Some researchers like [30] ignored the electrolyte diffusion dynamics to simplify the mathematical computation, which limits applicability of the model in high current condition. However, others consider the multiphase effect of the lithium ion batteries. In [32] modified boundary condition for electrolyte diffusion equation is proposed to decouple the PDEs.

Beside developing analytical or numerical solution for electrochemical models to find voltage current relation of the battery cell, Electrochemistry based impedance models are also proposed in which the equivalent impedance for each thermodynamic phenomenon is calculated from the electrochemistry of the cell. The models consider the electrochemical impedance due charge transfer reaction, diffusion in the electrodes, effect of ion concentration, double layer effect and insulation film growth. The electrical parameter values are calculated or determined from the physical parameters of the cell like diffusion coefficient, concentration in electrolyte and solid phase. Those types of model are less complex than numerically solved electrochemical models, and still retains some physical parameters of the cell.

2.2.2   **Equivalent Electric Circuit (EEC) Models**

Models based on equivalent electrical circuits are widely used in battery management and system level control algorithms due to their less computational effort. EEC is an empirical based model which contains active and passive electrical components to evaluate the battery performance. Varies equivalent circuit models are proposed in the literature. The choice of the equivalent circuit mainly depends on the battery chemistry and the level of detail characteristics considered. It depends on the trade-off needed between model accuracy and parameter identification simplicity. Figure 2-10 shows a typical representation of a battery cell impedance property with equivalent electric impedance elements. Charge transfer reaction, diffusion of lithium in the active electrode material and electrolyte, double layer effect and contact resistance between electrically conducting material are the main properties to be accounted for representing the battery characteristics in to electrical circuit equivalent [16]. This typical model assumes Solid Electrolyte Interface (SEI) film growth is only in the anode side and thin film in cathode side. Due to the rough electrode surface, the porous electrodes have a double layer effect with capacitance dispersion which better described by constant phase elements (CPE), a capacitance property with two degrees of freedom, instead of ideal capacitor. The diffusion dynamics of active materials in solid electrodes could be represented by Warburg impedance (W_a).
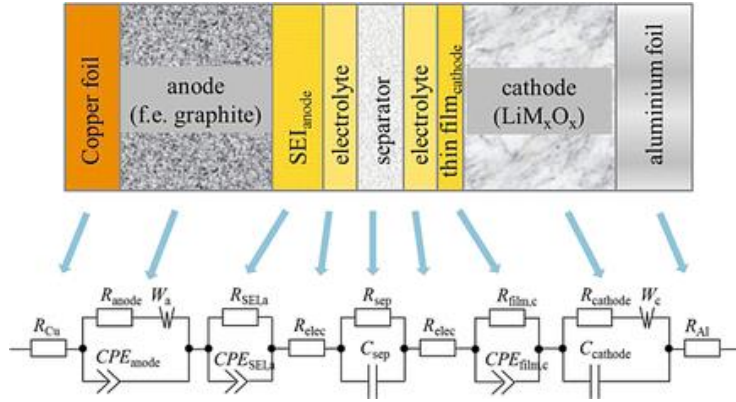
Figure 2-10 Typical equivalent circuit representation of cell components [8].

Representing all those impedance effects in EEM increase system and parameter estimation complexity, and models with less number of impedance elements are implemented in most applications by compromising system accuracy. Figure 2-11 shows simplified and compact representation which is known as Randel's model. To make the simulation of the model interactable Warburg impedance in the model can be represented by numbers of parallel RC branches. For exact equivalence of the transformation infinite number of RC networks are needed, however often finite numbers are used considering only certain frequency ranges. Effect of diffusion layer capacitance is small and often neglected in the model. Hence, the final model will have series electrolyte and charge transfer resistance with numbers of RC networks. Beside Randel's model, various topologies of those impedances interconnection in equivalent circuit form are also developed.
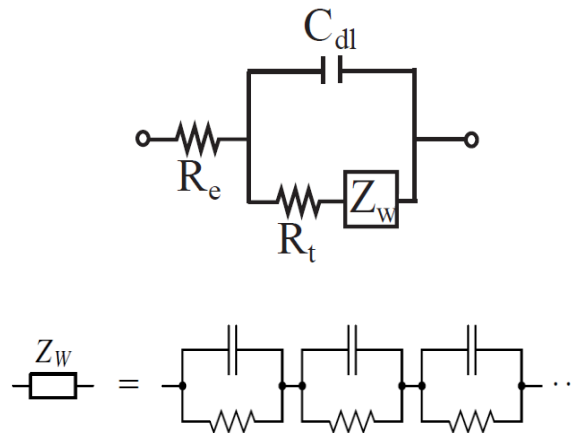
Figure 2-11 Randel's model

The objective of EEC modelling approach is trying to emulate the dynamic behavior of operating battery cell; hence any combination of impedances could be acceptable as far as it gives less computational and parameter estimation effort with acceptable accuracy for the dynamic performance in any operating conditions. The simplest model contains a voltage source and single resistor which represents the irreversible loss in the cell. First and second order Thevenin models, as shown in Figure 2-12, are widely used in BMS and other performance modelling applications. The model contains three main parts to have a better footprint of the battery cell; dependent voltage source to represent the open circuit voltage as a function of SOC, Ohomic resistance in series for electrolyte resistance and electrode conductivity, and one or more branch of parallel resistor and capacitor to approximate charge transfer and diffusion processes in the cell. The number of parallel RC branches can be determined from the empirical data of the battery cell using a curve fitting or other techniques. Two RC branches can give a good fit for most cell performances, however up to five RC branches could be used to capture the aging effect of the cell precisely [33] [34]. The SOC is calculated as voltage value across a capacitor in parallel with current dependent current source. The capacitance value is the maximum charge capacity of the battery cell in Ampere-second. A parallel resistance with the capacitor can also be considered to account self-discharge of the cell. Partnership for a New Generation of Vehicles (PNGV), a research cooperation in U.S. was also proposed another EEC model shown in Figure 2-13 [35], which is a Thevenin type model with a series capacitance to capture the variation of OCV with SOC. The relation between OCV with SOC can be also represented by lookup table without adding capacitance in series.
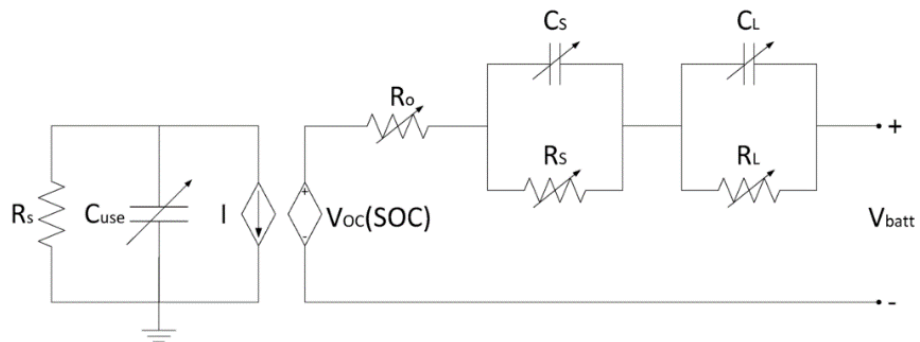
Figure 2-12 Two RC branch Thevenin model.
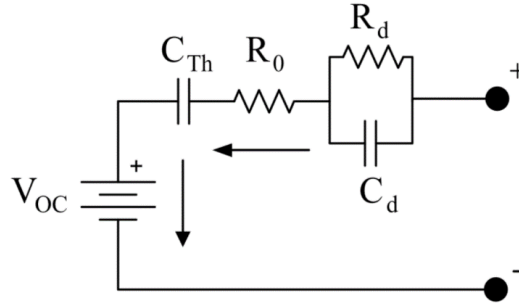
Figure 2-13 PNGV equivalent circuit model

2.3 Thermal Model of Lithium ion Battery

Temperature and voltage ranges are the key limiting factors of lithium ion battery. There is a safe temperature limit for each type of batteries on charge and discharge. Excluding some specialties, lithium ion batteries can be charged from 5 to 45°C and the permissible discharge temperature is from -20°C to 60°C [36]. At higher temperature charge and discharge performance is good but it affects the battery lifetime. The capacity and performance vary with the operating temperature and internal thermal conditions of the cell. Capacity of lithium ion batteries can decrease up to 95% when the battery is operating below -10°C compared with 20°C [37]. The state of health of the battery is also adversely affected by the battery temperature. To maximize the lifetime of the battery, temperature difference inside the cell should be less than 5°C [38]. Degradation effect of temperature on the battery cell parts are studied by different researchers. For instance, [39] discussed the effect of elevated temperature on the negative electrode (anode), thermal aging of the electrolyte and electrolyte-electrode interface is investigated by [40] and [41] [42] respectively. For a better battery thermal management regarding safety and lifetime, modeling thermal behavior of a battery at cell and pack level is essential.

Since operating temperature and thermal distribution inside have been found as a factor on the battery performance, different thermal modelling approaches are proposed in literature. Energy balance equations, heat generation equations and boundary condition for different heat transfer possibilities (radiation, conduction, convection) are the basic backgrounds to drive computational relation for thermal behavior of the battery. In [43] some of the thermal modelling methods are reviewed and compared in terms of computational intensity and accuracy. Computational and analytical thermal models from two-dimensional transient finite element analysis to lumped capacitance thermal models are based on the energy balance differential equations. Internal heat

generation is part of the energy balance equation which comes mainly from overpotential and entropy change of the system. Heat generation from overpotential depends on the operating temperature and current however heat generation due to change in entropy depends on state of charge of the battery. Lumped capacitance thermal modelling (one dimensional approach) considers the transient thermal distribution of the system is spatially the same and only depends on time which assumes transient conduction is much faster than heat transfer across the boundary of the system. For good approximation of the model the ratio of heat transfer resistance inside and at the surface which is known as Biot number should be much less than 1(i.e. $B_i = \frac{hL_c}{k} \ll 1$ where Bi is Biot number, h is convection heat transfer coefficient-W/mK, Lc length of the system across the heat transfer-m, k is conduction heat transfer coefficient- W/m^2K). However, in two-dimensional finite element analysis based model the spatial thermal distribution of the system is considered based on the material involved inside it which will be governed by differential equations and the problem will be solved using finite number of elements by minimizing the error. Detailed analysis of both methods and other approaches are discussed in depth in the above reference.

2.4 Data Measurement Techniques for EEC Models Parameter Estimation

Parameters of EEC model are estimated either using frequency domain or time domain data points. To have frequency domain data of the battery cell, Electrochemical Impedance Spectroscopy (EIS) is the popular impedance measuring device for electrochemical systems. The internal impedance of the cell is measured for a frequency range of *mHz* to *kHz* to capture slow and fast system dynamics. Time domain analysis is done from recorded terminal voltage using charging/discharging current pulses with proper relaxation. If simple battery model is appropriate for the application, electrical parameters of the EEC model can be extracted from manufacture datasheet values and graphs, like in [44], though the model will not be accurate enough regarding its transient behavior. The accuracy of EEC model highly depends on how the battery cell is exercised during experimental data collection. Batteries degrade because of usage, life cycle stress and other stability conditions. Destructive and nondestructive measurements can be done to observe the degradation characteristics of the battery. Electrical characterization tests such as EIS, charge/discharge cycling and OCV are nondestructive measurements. Furthermore, the internal structure of the battery can be explored through ultrasonic transduction, neutron imaging, and X-ray microscopy. Destructive tests need stripping the cell and directly observing changes in the electrode morphology [45].

2.4.1 Frequency Domain Measurement – EIS Characterization Technique

EIS has been used to characterize the electrochemical dynamics of batteries and other electrochemistry based systems for measuring the electrochemical impedance at different frequencies. The electrochemical impedance is usually measured by applying AC voltage (DC voltage is also possible) to the system and measuring the current or the vice versa. For non-linear system like lithium battery the applied AC signal should be small to treat the response as a linear system. As shown in equations 2-18 and 2-19, voltage E(t) can be measured for battery cell current I(t). From Ohms law, the ratio of the voltage to the current is a complex relation with amplitude and phase which represents the impedance effect of the cell. Equation 2-20 and Figure 2-14 explains this voltage-current relation.

$$E(t) = E_0\sin(\omega t) \qquad\qquad (2\text{-}17)$$

$$I(t) = I_0\sin(\omega t - \phi) \qquad\qquad (2\text{-}18)$$

Where, $\omega = 2\pi f, f$ is the frequency of voltage and current applied.
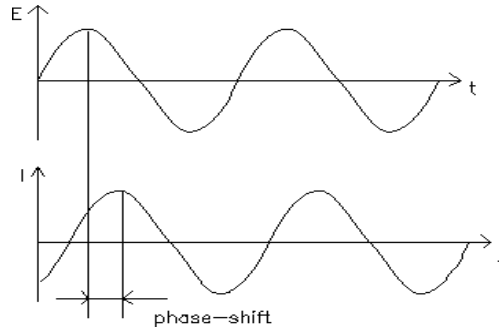
Figure 2-14 AC voltage and current for EIS [46]

$$Z(t) = \frac{E(t)}{I(t)} = \frac{E_0\sin(\omega t)}{I_0\sin(\omega t - \phi)} = Z_0\frac{\sin(\omega t)}{\sin(\omega t - \phi)} = Z_0(cos\phi + jsin\phi) \qquad (2\text{-}19)$$

EIS impedance data may be represented either in Nyquist or Bode plot. Having the EIS response of the electrochemical system, the data is compared with the equivalent circuit response for calculation of passive electric circuit elements. In Nyquist plot, real and imaginary part of the impedance is represented by a point at a single frequency which is not shown explicitly. However, in bode plot the magnitude and phase of the impedance response is represented in different plot,

and the frequency is explicit. Electrical behavior of simple electrochemistry shown in Figure 2-15 as Randel's electric circuit can be approximated using a double layer capacitance, electron transfer resistance and uncompensated electrolyte resistance. The horizontal distance of the semicircle from the imaginary axis represents the series resistance. If the impedance characteristic is as shown in Figure 2-17, the data can be fitted by Randel's equivalent model with Warburg impedance. At low frequency, the impedance has a constant phase which can be modelled by Warburg impedance, $\frac{A_w}{(j\omega)^{1/2}}$ where A_w is the Warburg coefficient and ω working frequency. At the middle frequency, the Nyquist plot is semi-circular approximated by parallel resister capacitor network. When the frequency gets higher and higher the imaginary part of the impedance becomes negligible which has only resistive property. At higher frequencies, the Nyquist plot might have negative imaginary part also which shows the inductive property of the cell. Adding resistor-inductor parallel network or other possible combination of resistors and inductors in the equivalent circuit will handle this characteristic. Detailed explanation of EIS technique for modeling different electrochemical system is found in [46]. The electrochemical impedance should be measured at different operating conditions i.e. Temperature, SoC and Capacity rate to get the impedance footprint of the battery cell at those conditions. Curve fitting technique is applied to estimate electrical parameters of each branches of the Nyquist plots.
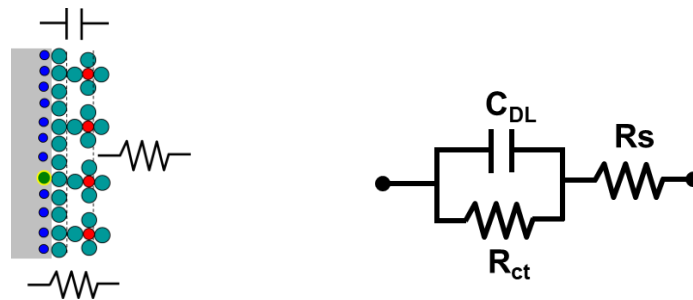
Figure 2-15 Simplified Electrochemistry and Equivalent Randle's Circuit [47]
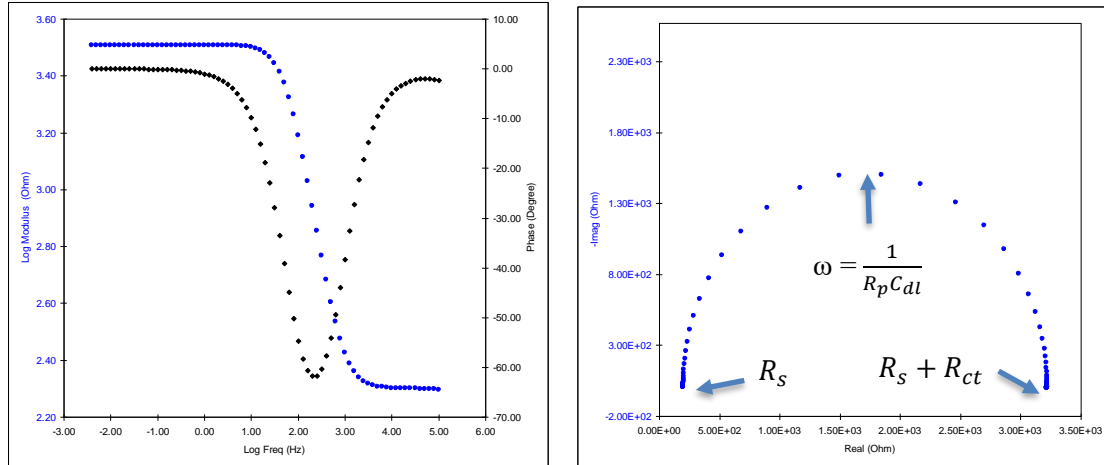
Figure 2-16 Bode and Nyquist plot from EIS [47]
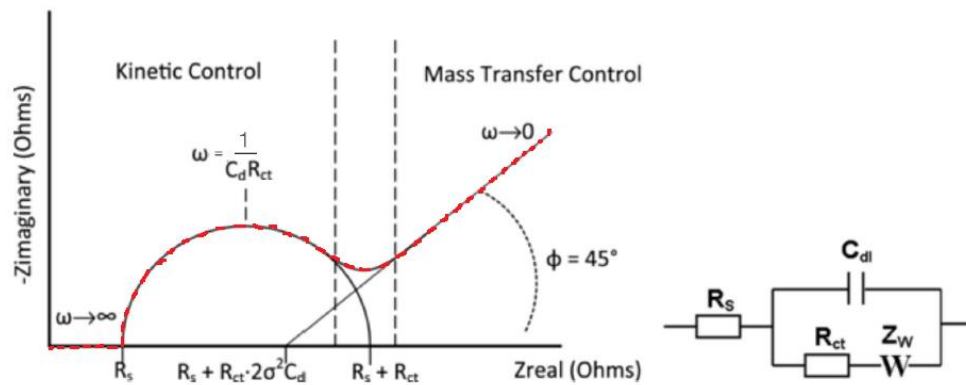
Figure 2-17 Typical Nyquist plot and electrical circuit equivalent of each subpart

2.4.2 Time Domain Measurement - Measuring Terminal Voltage from charge/discharge Current

Data of dynamics for the battery cell can be also extracted from the pulsed and relaxed terminal voltage response. A pulse charge/discharge current is applied to the cell and terminal voltage is measured. The battery cell can be exercised using different charge-discharge strategies. Pulse charge-discharge, HPPC, DST are common methods [48]. Figure 2-19 shows a typical pulse discharge pulse and relaxation voltage response. If response is zoomed as in Figure 2-20, the system impedance can be approximated by a resister in series with RC elements. series equivalent resistance of the cell is estimated from the voltage step ΔV_1 using Ohm's law: $R_0 = \frac{\Delta V_1}{I}$ where I, is the magnitude of discharge current. The transient part of the voltage response ΔV_2 can be

29

approximated by one or more numbers of parallel RC branches. Thermal effect of the system can be captured by performing the experimental test at different operating temperatures. During modelling, the electric circuit parameters should be estimated and a relation should be developed. Lookup table and exponential nonlinear equations are used, however the first one is more convenient.

(a)   (b)
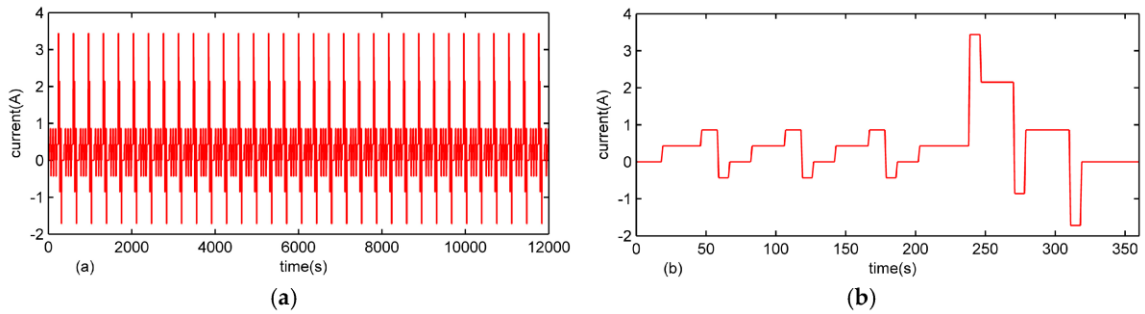
Figure 2-18 (a) Typical HPPC test profile for full SoC range (b) HPPC test profile at specific SOC
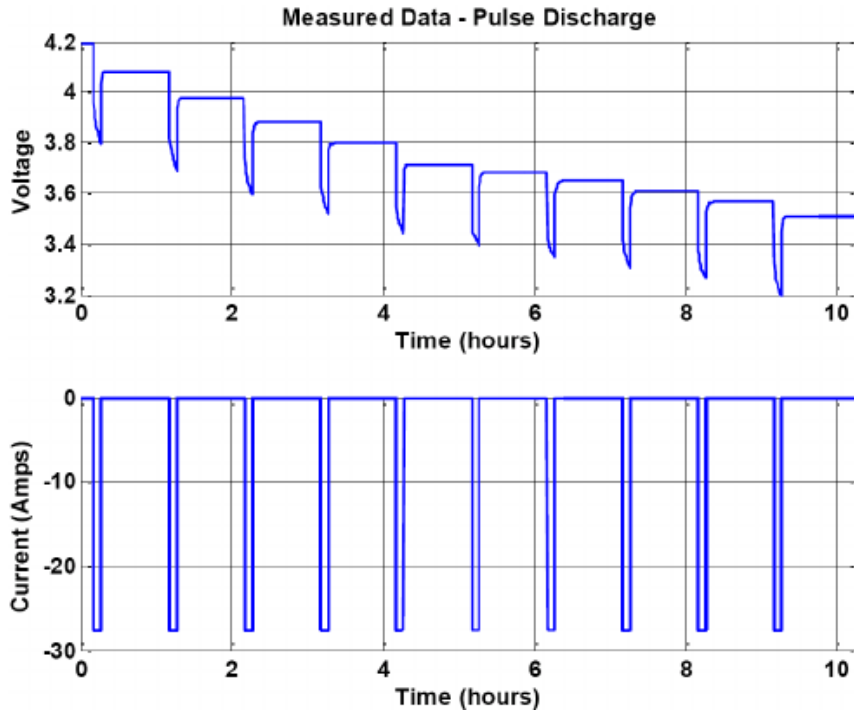
Figure 2-19 Pulse discharge test
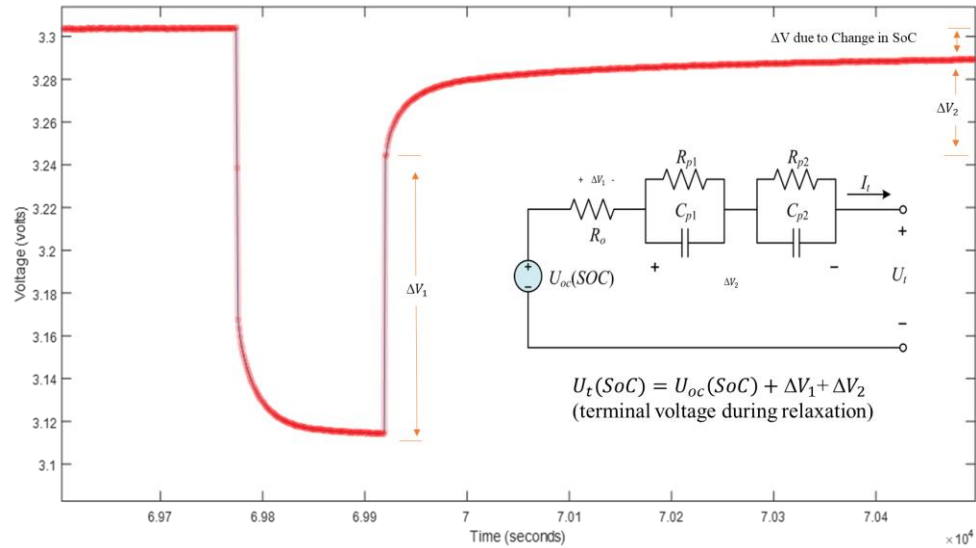
Figure 2-20 Terminal voltage response of a battery cell for pulse discharge current and relaxation

2.5 SOC Estimation Techniques

SOC is a measure of the remaining capacity of the battery cell with respect to a reference capacity, usually the nominal capacity of the cell. A nominal capacity is a value given by the manufacturer which represents the maximum amount of charge can be stored in the cell. However, this definition is not always true since the capacity of the cell varies at different operating temperature and cell age. Open circuit voltage and cell impedance parameters have nonlinear relation with SOC. Estimating SOC is a challenge in battery world since there is no direct way to measure it. It is also a very important parameter for battery control strategy in BMS. Determining SOC of the cell through the operating range is also vital for battery modelling accuracy. Various techniques are proposed to estimate SOC from the simplest and most famous one, Coulomb counting to Adaptive methods based on Artificial intelligent techniques.

2.5.1 Coulomb Counting (Book keeping) Method

The remaining capacity can be calculated by accumulating the charge transferred in and out of the battery during charge and discharge. This calculation is needs knowing the initial capacity of the cell. SOC is expressed in percentage form as shown in equation 2-21 below by integrating the charge/discharge current through the operating range and accumulating the value in a memory, where C_n is nominal capacity and η is the columbic efficiency. This technique highly relied on the

current measurement accuracy and initial SOC estimation. Because of the integrator, the error accumulates, and the estimated value may drift from the real SOC if the measurement noise is significant. However, due to the simplicity it is implemented in most BMS, battery modelling and other battery performance analysis.

$$SoC(t) = SoC_0 - \frac{\eta}{C_n} \int_{t0}^{t} i(t)dt \qquad (2\text{-}20)$$

2.5.2   Open Circuit Voltage (OCV) Based

State of charge can be also estimated from the voltage measurement, which is nonlinear relation between open circuit voltage and SOC as shown in Figure 2-21. The voltage measurement is approximated by nonlinear function or a lookup table and implemented for SOC prediction. However, the estimation may be inaccurate because of the battery voltage varies with temperature and operating rate. Measuring the open circuit voltage is not also an easy task which needs long relaxation time after discharge or charge for corresponding SOC calculation point. The voltage characteristics has also hysteresis effect during charge transfer which influences the estimation accuracy. Some lithium battery technologies have also flat SOC-voltage relation which makes using this technique inefficient for those types of batteries.
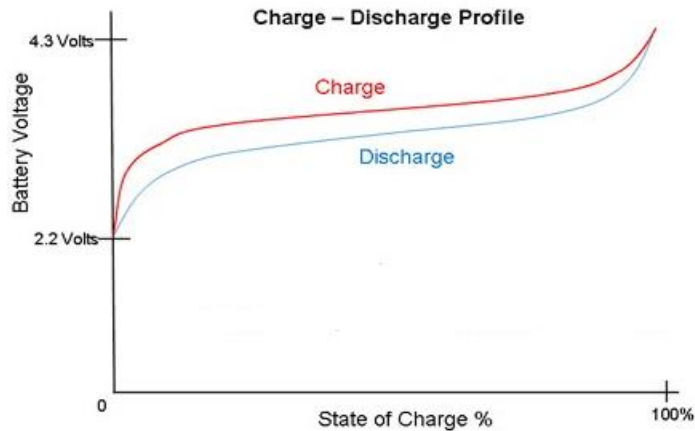
Figure 2-21 Charge-discharge SoC voltage relation

2.5.3   Adaptive Methods (closed loop):

Several adaptive techniques such as Kalman filter, Fuzzy logic, Neural network or other recursive methods are proposed for SoC estimation. These techniques have better accuracies due to their closed loop strategy.

Kalman Filters (KF): KF is an algorithm extensively used in system control and performance analysis for estimating unmeasured states of the system. It is robust in handling measurement uncertainties and system disturbances. The algorithm has state predicting and correcting stages. It assumes a linear Gaussian state space relation of the system. It is not efficient for nonlinear state space model and non-gaussian disturbance distribution. However, it has different variants to support nonlinear systems: Extended Kalman Filter (EKF) and Unscented Kalman Filter (UKF). In EKF the system, state space model is approximated by Gaussian random variable and the nonlinear system model is approximated by first order linear model using Taylor series propagation. The approximation may lead to large error or divergence of the actual and estimated state variables if the noise distribution is far from Gaussian or due to the first order approximation. UKF algorithm improves the efficiency by using deterministic sampling approach instead of first order approximation of the nonlinear system. The system distribution is represented by sample points which completely captures the system mean and covariance.

Kalman filter based algorithms require state space representation of the cell model as state and output equations in discrete form.

$$x_{k+1} = f(x_k, u_k, w_k) \tag{2-21}$$

$$y_k = g(x_k, u_k, v_k) \tag{2-22}$$

Where x is state variables and y output variables, f is transition matrix and g is measurement matrix, w and v are system and measurement noises respectively. Though specific state space representation for SOC estimation depends on the type of battery cell model chosen, basically it includes coulomb counting based SOC equation with state disturbance as state equation and cell terminal voltage/OCV relation with measurement noise as output equation to formulate the state space model. For instance, for EEC model with series resistor and 2-RC networks the state space model can be formulated as:

$$SOC_{k+1} = SOC_k - \frac{\eta i_k \Delta t}{C} + w_k \tag{2-23}$$

$$V_k = OCV(SOC_k) + v_{R0} + v_{RC1} + v_{RC2} + v_k \tag{2-24}$$

The output equation V_k requires the relation between OCV and SOC which is a challenge in SOC estimation process. Various approaches from linear to more complex relations are proposed in literature, the one shown in equation 2-25 is known as Nernst Model [49].

$$OCV(SOC_k) = K_0 - \frac{K_1}{SOC_k} - K_2 SOC_k + K_3 \ln(SOC_k) + K_4 \ln(1 - SOC_k) \qquad (2\text{-}25)$$

Where;

$$x_k = SOC_k, y_k = V_k, u_k = i_k \qquad (2\text{-}26)$$

In EKF algorithm, the state space equation should be linearized and approximated by first order equation as a general form.

$$x_{k+1} = Ax_k + Bu_k + Qw_k \qquad (2\text{-}27)$$

$$y_k = Hx_k + Rv_k \qquad (2\text{-}28)$$

Where A is state matrix, B input matrix, H output matrix, Q system error covariance matrix, R measurement error covariance matrix, P estimation error covariance, and K is Kalman gain. The implementation of the algorithm has two basic steps, prediction and correction stages.

Prediction Step (Time Update):

$$\hat{x}_k^- = A\hat{x}_{k-1}^- + Bu_{k-1} \qquad (2\text{-}29)$$

$$P_k^- = AP_{k-1}A^T + Q \qquad (2\text{-}30)$$

Kalman Gain Calculation:

$$K_k = P_k^- H^T \left(HP_k^- H^T + R \right)^{-1} \qquad (2\text{-}31)$$

Correction Step (Measurement Update):

$$\hat{x}_k = \hat{x}_k^- + K_k (y_k - H\hat{x}_k^-) \qquad (2\text{-}32)$$

$$P_k = (I - K_k H)P_k^- \qquad (2\text{-}33)$$

The algorithm needs also the initial estimates of the state $(\hat{x}_0^-)$ i.e. SOC_0 and the state error covariance matrix P_0^-. Detailed information of using Kalman filters for SOC estimation is found in [1] and [5].

Artificial Neural Network: it is an artificial intelligent technique with a mathematical model consists of interconnected artificial neurons to estimate the dynamics of a system based on some historical data that is taken from experiments. ANN has hidden, input and output layers. The number of hidden layer may be any number; however, two hidden layers are usually enough to train most of the dynamic systems. One hidden layer is also good enough to capture the system dynamics. Each layer contains nodes. The nodes in the hidden layers have activation functions which transform the input signal into output signal. The layers are connected by weights which will be determined during the training of the neural network based on function minimization. Those weight values contain information about the dynamics of the trained system. Two configurations of ANN are available: Feedforward or Feedback configuration. In feedforward signals travel only in forward direction however in feedback ANN signals also travel backward from output to input neurons. In literature ANN is proposed to estimate SOC for battery management system. Data for the training can be collected from the battery charge discharge profile under different working conditions including temperature and capacity rate. Though it is highly data and training dependent, some researchers claim as it has better dynamic performance and stability for SOC estimation. In [50], ANN is compared with Kalman filter and the author showed EKF performs good if the battery and noise models are accurate and ANN perform good if the training is accurate.
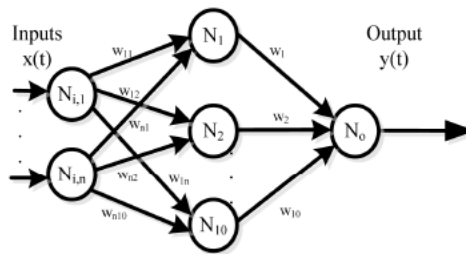
Figure 2-22 ANN with one hidden layer and an input output layer [50]

Chapter 3

Methodology

This chapter contains the methods applied to model lithium ion battery cell based on experimental data measured in the lab. It consists the proposed model, experimental setups and test profiles. Estimated parameters and simulation model are also presented.

3.1 Performance Model Structure
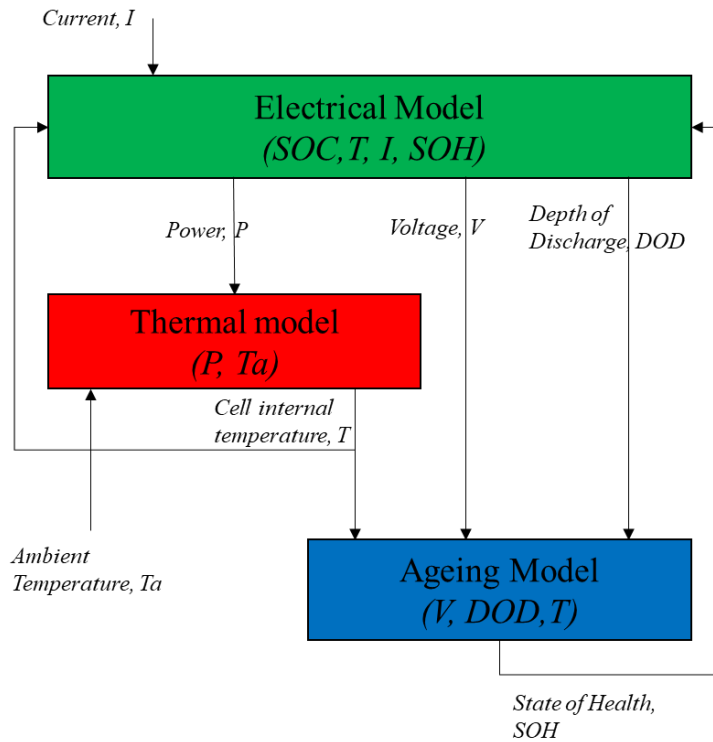
Figure 3-1 Typical battery cell model structure

Performance model of a lithium ion battery cell includes electrical, thermal and aging behaviors. Figure 3-1 explains a typical interaction of those three models to simulate those behaviors. The electrical model simulates voltage-current characteristics of the cell as a function of SOC, internal temperature, current rate and its state of health (SOH). The thermal model predicts the cell internal temperature considering current rate and working temperature. SOH of the cell is calculated from the aging model which is a function of depth of discharge (DOD) profile and cell temperature. The

main challenge in lithium battery cell modelling is the physical parameters in it are coupled and vary nonlinearly with the operating temperature, current rate and state of charge of the cell. In this work, the effect of working temperature (T), current rating (I) and variations with SOC is modelled empirically. Experimental tests are done to capture those effects from the battery cell terminal voltage-current relation.

3.2 Proposed Model

Temperature dependent EEC based model of a lithium ion battery cell is proposed as shown in Figure 3-2. The electrochemical impedance characteristics of the cell is approximated by electrical circuit elements. OCV is modelled with a variable voltage source to handle the variation SOC and temperature. Instantaneous voltage-drop or rise of the cell during discharge and charge is modelled with a resistor connected in series with OCV. The resister represents the electrolyte and current collector resistive effect in the cell. Time dependent voltage change due to charge transfer and mass transport inside the cell is captured with parallel RC circuits. A single or more RC circuit network can capture dynamic behavior of the cell. Curve fitting techniques are applied to determine the number of parallel RC circuits for capturing the system dynamics with high fidelity and low parameter estimation complexity based on preliminary experimental data. Table 3-1 shows curve fit comparison results with different number of RC elements on MATLAB curve fitting tool. Single RC element is not good enough to handle the fast dynamics and shows high residual error. More than one RC elements have good fitting. Fitting accuracy increases with number of RC impedance elements however number of parameters to be estimated increase. Sum Square Error (SSE), Root Mean Square Error (RMSE) and number of parameters (coefficients) are considered for comparison. Three RC parallel elements are considered to model electrothermal behavior of the cell with a trade of between fitting accuracy and parameter estimation. Considering the proposed model, on discharge cell terminal voltage V_t and current I_{dis} are related as shown in equation 3.4, where V_{oc} is OCV, V_0 , V_1, V_2 and V_3 voltage drops on impedance elements.

$$\dot{v}_1 = \frac{i}{C_1} - \frac{v_1}{R_1 C_1} \tag{3-1}$$

$$\dot{v}_2 = \frac{i}{C_2} - \frac{v_2}{R_2 C_2} \tag{3-2}$$

$$\dot{v}_3 = \frac{i}{C_3} - \frac{v_1}{R_3 C_3} \tag{3-3}$$

$$V_t = V_{oc} - v_0 - v_1 - v_2 - v_3 \qquad (3\text{-}4)$$

$$V_t = V_{oc} - I_{dis}R_0 - I_{dis}R_1\left(1 - e^{-t/R_1C_1}\right) - I_{dis}R_2\left(1 - e^{-t/R_2C_2}\right) - I_{dis}R_3\left(1 - e^{-t/R_3C_3}\right) \qquad (3\text{-}5)$$
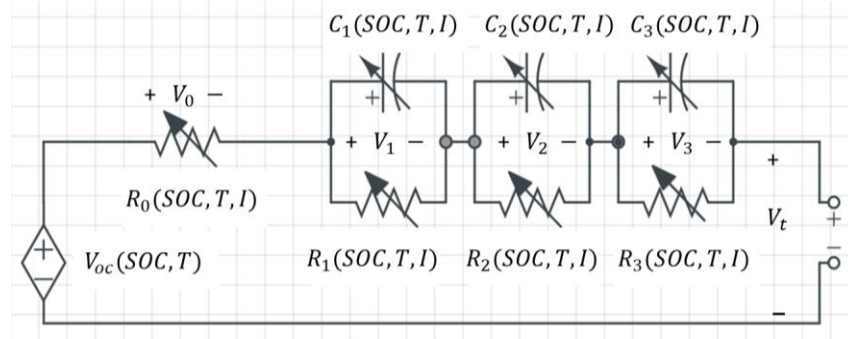
Figure 3-2 Proposed EEC battery cell model
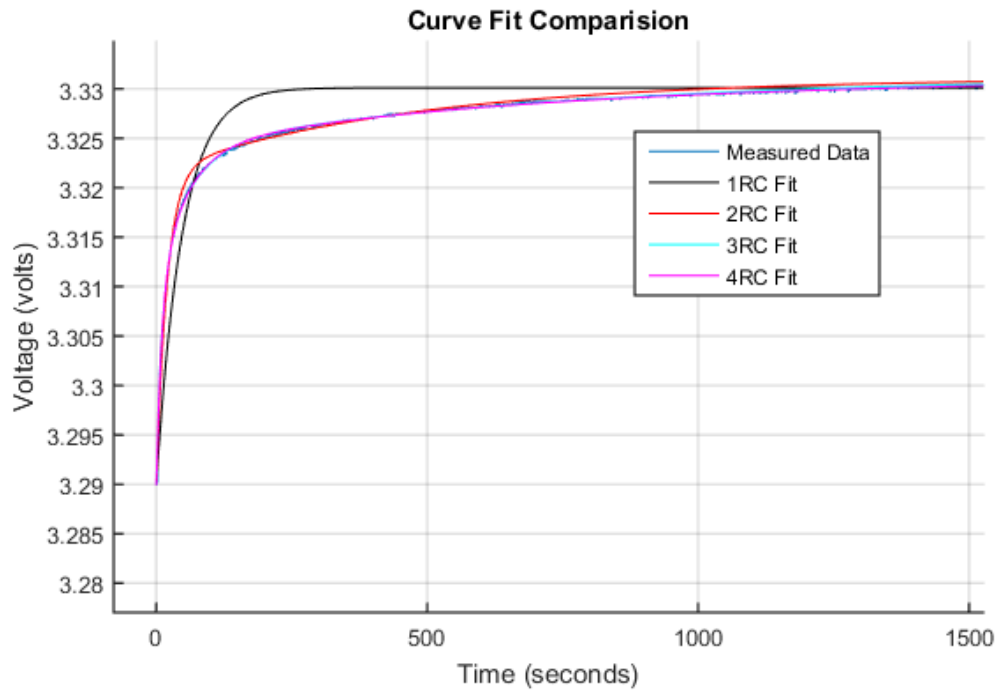
Figure 3-3 Experimental data and 1RC, 2RC, 3RC and 4RC model curve fit

Table 3-1 Curve fit results comparison

Model RC Networks	SSE	R-Square	RMSE	Number of Coefficients
1 RC	0.0106	0.7034	0.0017	2
2 RC	5.6052e-4	0.9843	3.9464e-4	4
3 RC	1.2884e-4	0.9964	1.8924e-4	6
4 RC	9.2893e-5	0.9974	1.6075e-4	8

SOC estimation is the backbone of the model, Coulomb counting technique is implemented as shown in Figure 3-4 using variable capacitor based electrical circuit. The capacitance of the capacitor represents the maximum Amp-second (maximum cell capacity) which is a function of temperature. The self-discharge and hysteresis effect of the cell is ignored in the model to minimize model complexity and their effect is little.

SoC interms of voltage :
$SoC(t)=SoC(t0)-1/C(T)\int idt$
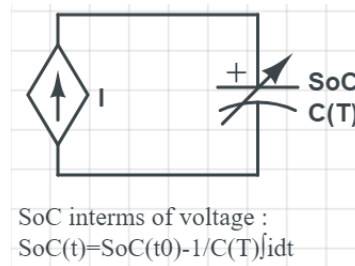
Figure 3-4 SOC estimation circuit

3.3 Experiment Setups

Battery test experiment is done using BaSyTec battery test platform in Cegasa Portable Energy battery test laboratory. Temperature chamber is used to control the ambient temperature during the test. The setup is as shown in Figure 2-1.

Figure 3-5 BaSyTec Battery test system

The experiment is time domain based which captures the transient voltage characteristics of the cell at different temperature (T), current (I) and SOC. The battery test device has enough technical resolution and precision to capture the cell dynamics which is detailed in Table 3-2 below.

Table 3-2 BaSyTec battery test system specifications [51]

Type	25A
Resolution	0.1mV/1mA
Precision	1mv/50mA upto 25A
	100mA per each 50A
Time resolution	1μs
Rise time	2ms
Minimum pulse length	10ms

The experiment includes static capacity and dynamic tests for impedance parameter and SOC estimations. Both tests are done using LFP lithium ion battery cell. The cell major technical specifications are attached in the appendix section of this paper.

3.3.1 Static Capacity Test

The purpose of the test is to calculate the maximum capacity of the cell at the required working conditions. The test is performed in the following procedure:

1. Use a new battery cell and fully charge it with Constant Current Constant Voltage (CCCV) method.
2. Discharge the cell with 0.5C current rate (manufacturer recommended value)
3. Repeat charge-discharge cycle until the capacity stabilizes with less than 1% change after three cycles, if the cell is new. The cell capacity increased slightly for the first few cycles because of the solid electrolyte interface (SEI) effect in the new cell.
4. Calculate the maximum capacity.

Maximum capacity of the cell varies with working ambient temperature. Capacity test is performed at different temperature which considered as break points in the modelling.

3.3.2 Dynamic Test

In the dynamic test, the transient voltage characteristics of the cell is measured at various working conditions. During the test, up to 1C on charge and 3C on discharge maximum current rates are considered. Those values are given as the maximum current limitations on charge-discharge of the cell by the manufacturer of the cell under experiment.

From fully charge condition of the cell, current profile as shown in Figure 3-6 is applied. It is a customized HPPC profile. Terminal voltage of the cell is recorded with 1-second voltage resolution. 0.2C, 0.5C, 1C, 2C, 3C discharge and 0.2C, 0.4C, 0.6C, 0.8C, 1C charge current pulses are considered. The experiment is repeated at all temperature break points (i.e. 0°C,10°C, 20°C, 30°C, 40°C) and SOC break points (i.e. 100%, 98%, 94%, 90%, 80%, 70%, 60%, 50%, 40%, 30%, 20%, 10%, 6%, 4%, 2%, 0%) considered. The customized HPPC current profile is summarized as:

1. Discharge the battery cell with 0.2C for 20 seconds and pause it for 1hour (relaxation time for the electrochemical reaction).
2. Charge it with 0.2C for 20 seconds and pause 1hour.
3. Discharge it with 0.5C for 20 seconds and pause 1hour.
4. Charge it with 0.4C for 25 second and pause 1hour.
5. Discharge it with 1C for 20 seconds and pause 1hour.

41

6. Charge it with 0.6C for 30 second with and pause 1hour.

7. Discharge it with 2C for 20 seconds and pause 1hour.

8. Charge it with 0.8C for 50 second and pause 1hour.

9. Discharge it with 3C for 20 seconds and pause 1hour.

10. Charge it with 1C for 60 second and pause 1hour.

11. Then discharge the cell with 0.5C to the next SOC breakpoint

12. The test is repeated for different temperature points to capture the temperature effect.

From the measured terminal voltage, OCV-SOC relation is also calculated. Voltage value at the end of the relaxation time is considered as OCV, assuming the cell fully recovered from polarization during discharge/charge.
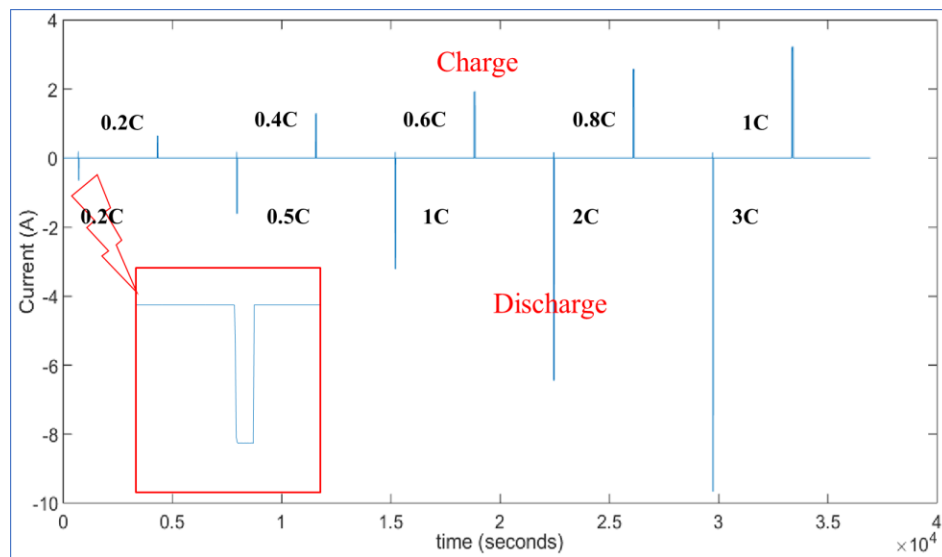
Figure 3-6 Battery cell dynamic test current profile

3.4 Data Analysis and Parameter Estimation

The measured data shows that the cell voltage characteristics varies due to temperature and SOC variation. Figure 3-7 is terminal voltage recorded during HPPC test at 10°C and 40°C. This is mainly due to change of OCV and cell impedance parameters. Therefore, this variation of impedance parameters should be estimated and included in the model.

42
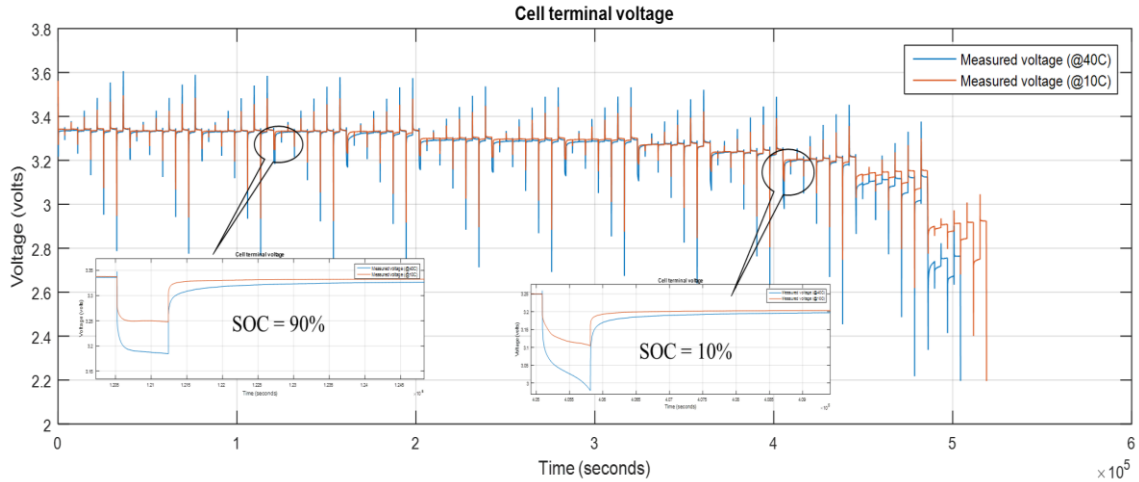
Figure 3-7 Cell terminal voltage during dynamic test at 10°C and 40°C

Hence, the main task in EEC modelling is the parameter estimation step for the proposed model. Least square (LS) minimization method is common to find optimal parameters of a model either based on sum squared or absolute error. In LS problem, the sum of the square of the errors between the measured data points and the model function values is minimized iteratively by updating the model parameters. In this work MATLAB/Simulink optimization tool is used to estimate impedance parameters. It has various optimization methods and algorithms implemented within it. Gradient descent, Nonlinear least square, pattern and simplex searches are the algorithm methods included. The algorithm might be Levenberg-Marquardt, Trust-region-Reflective or other. Levenberg-Marquardt is a standard technique to solve non-linear least square problems. It is a curve fitting method combining two minimization methods; the Gradient decent and Gaussian methods. Gradient descent method minimizes the sum of the squared errors by updating the parameters in the steepest-descent direction. However, Gauss-Newton method minimize the sum of the squared errors by assuming the least squares function is locally quadratic, and finding the minimum of the quadratic. The Levenberg-Marquardt method is more like a gradient-descent method when the parameters are far from their optimal value, and acts more like the Gauss-Newton method when the parameters are close to their optimal value. The problem formulation and numerical implementation of the algorithm is detailed in [22]. Trust-region-Reflective is a minimization approach based on trust region, not a line search algorithm. Here, the problem is approximated by a simple function within the neighborhood of the data point, and that neighborhood is the trust region. This trust region is adjusted from iteration to iteration. If the approximated model fits the

43

original problem well the trust region can be enlarged, otherwise if the approximation is bad the trust region should be reduced. The method is strongly associated with approximation [52]. Levenberg-Marquardt method has a limitation of handling bound constraints and Trust-region-Reflective methods doesn't solve undetermined systems. Figure 3-8 shows some windows of the graphic user interface of MATLAB optimization toolbox. Parallel pool option in the toolbox is also selected during estimation to use all local works in the computer which makes the estimation process faster. Trust-region-Reflective is chosen as optimization method since the impedance parameters to be estimated are bounded. The resistance and capacitance values should be greater than zero which enforce bounded constraints in the optimization problem. Since the training data for the whole SOC range is big, the parameter estimation is done separately for each SOC break points separately and finally the estimated parameters are collected. Detail explanation of how to use MATLAB optimization toolbox to estimate parameters in a Simulink model is explained in the toolbox user's guide [53].

Figure 3-8 MATLAB Optimization Toolbox GUI snapshot

44

3.5 Simulink Implementation of the Model

3.5.1 Model Subsystems

Simulation model of the battery cell is as shown from Figure 3-9 to Figure 3-11. The model consists of three parts: impedance, SOC estimation and OCV model. The impedance subsystem is variable resistor and capacitor elements with 3D lookup tables.
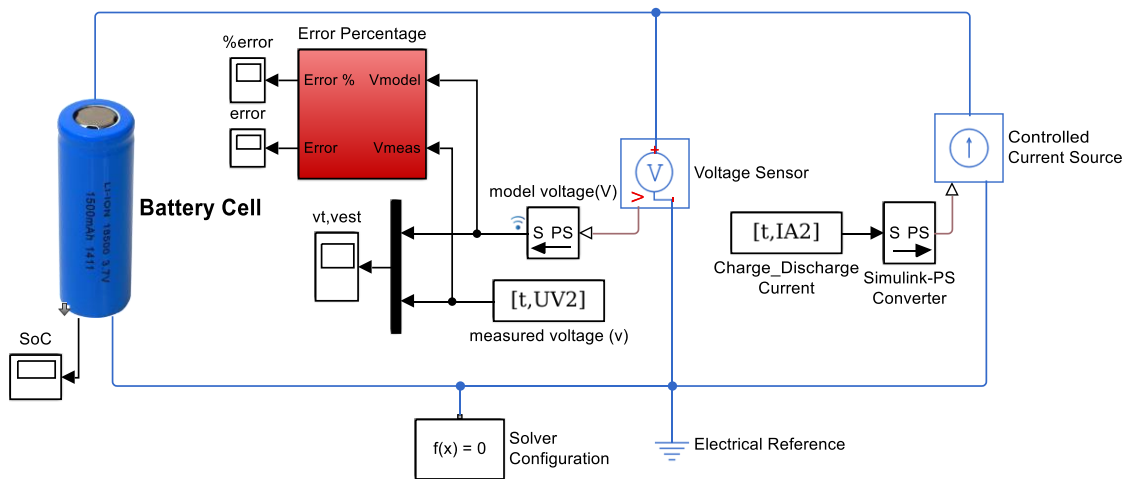
Figure 3-9 Model top level system
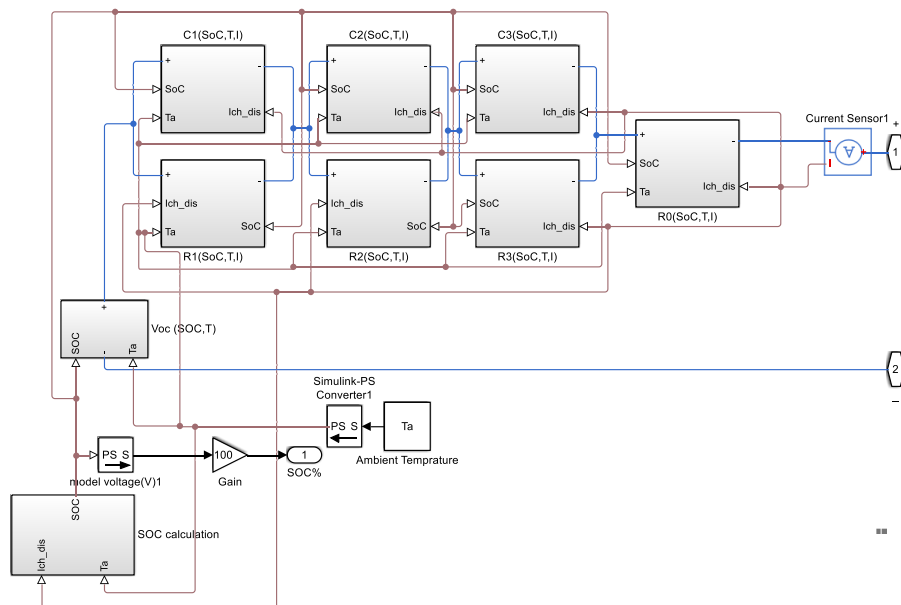
Figure 3-10 Model subsystems
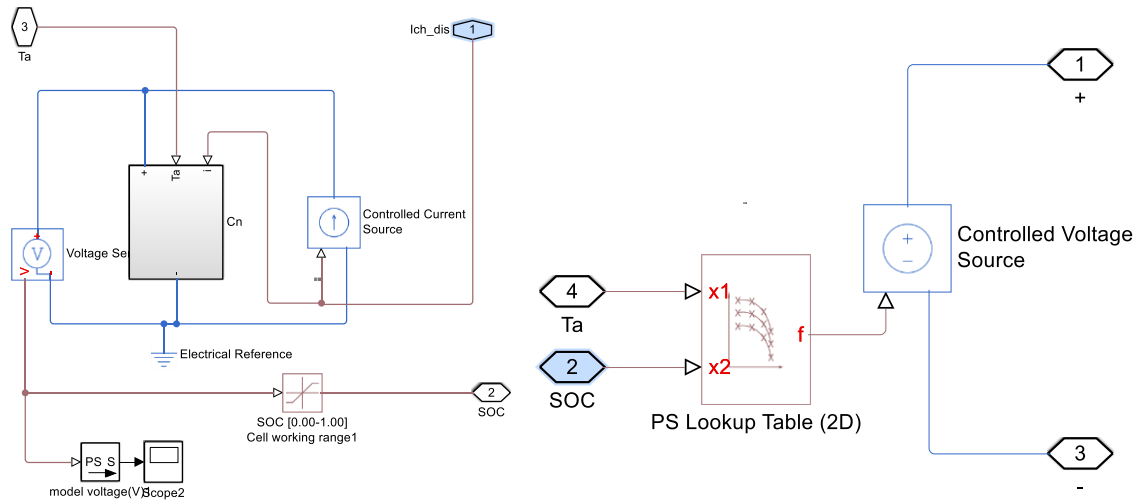
Figure 3-11 OCV and SOC estimation subsystems detail

It is also applicable to connect the cell model in parallel or/and series and simulate battery pack level behavior, but in this work the model is not validated for battery pack level which will be done in the future work.
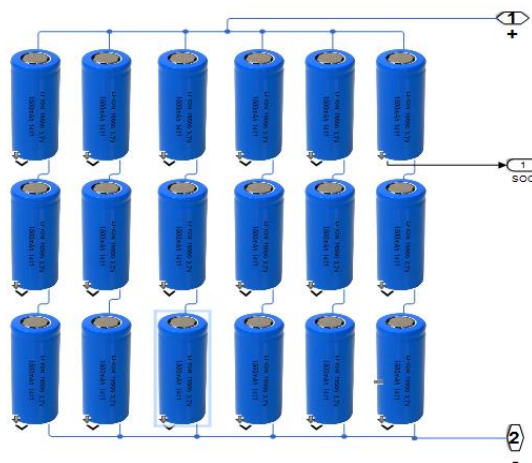
Figure 3-12 6X3 cell battery pack model

The model also has mask parameters or graphic user interface (GUI) as shown in Figure 3-13. It helps to change model parameters easily, like change the initial state of charge and ambient temperature and capacity of the battery cell.

46
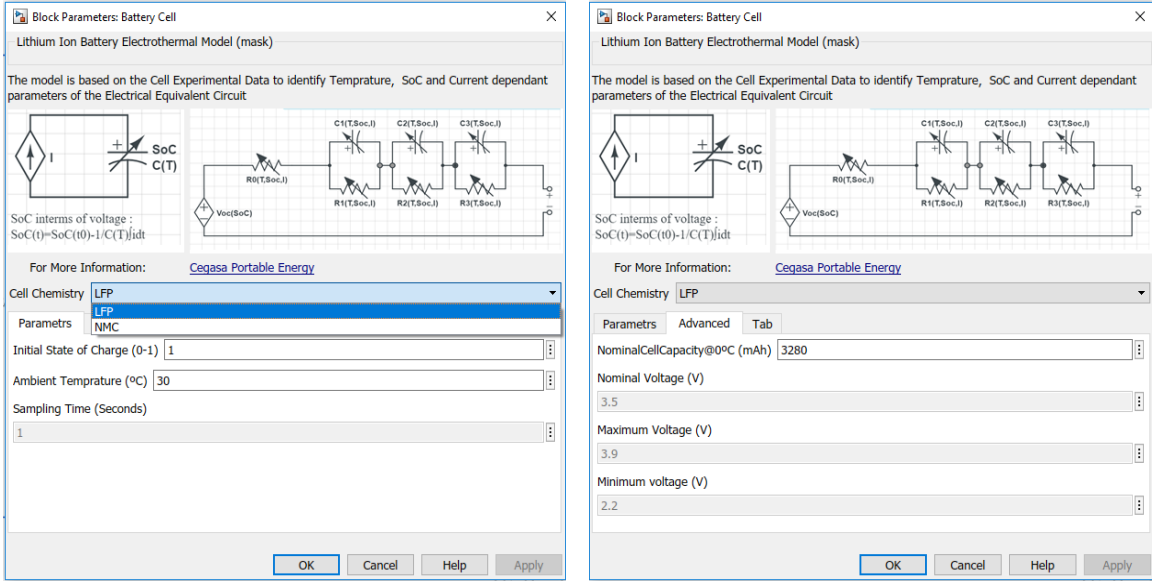
Figure 3-13 Model GUI (parameter mask)

3.5.2 Estimated Parameters

Maximum Cell Capacity: Maximum cell capacity as a function of temperature which is extracted from static capacity test is described in Table 2-1. It shows that the cell capacity increases with ambient temperature.

Table 3-3 Maximum cell capacity at different temperature

Temperature (C)	Max. Cell Capacity (mAh)	Equivalent Capacitance (F)
0	3250	11700
10	3300	11880
20	3310	11916
30	3318	11945
40	3360	12096

OCV: open circuit voltage of the cell is collected from the dynamic test at each SOC and ambient temperatures is plotted as 2D graph shown below in Figure 3-14 and Figure 3-15. From fully charge

up to 35% SOC, higher temperature has higher OCV value. However, this is not true when SOC goes below that.
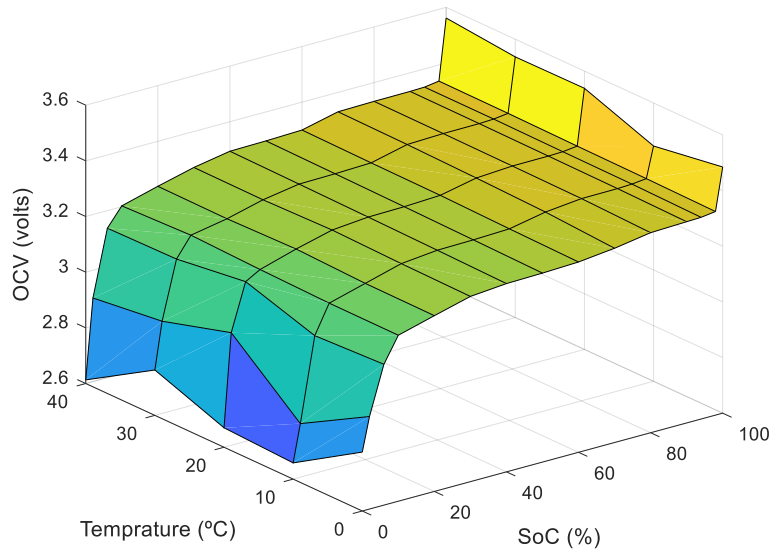
Figure 3-14 2D plot of OCV as a function of temperature and state of charge
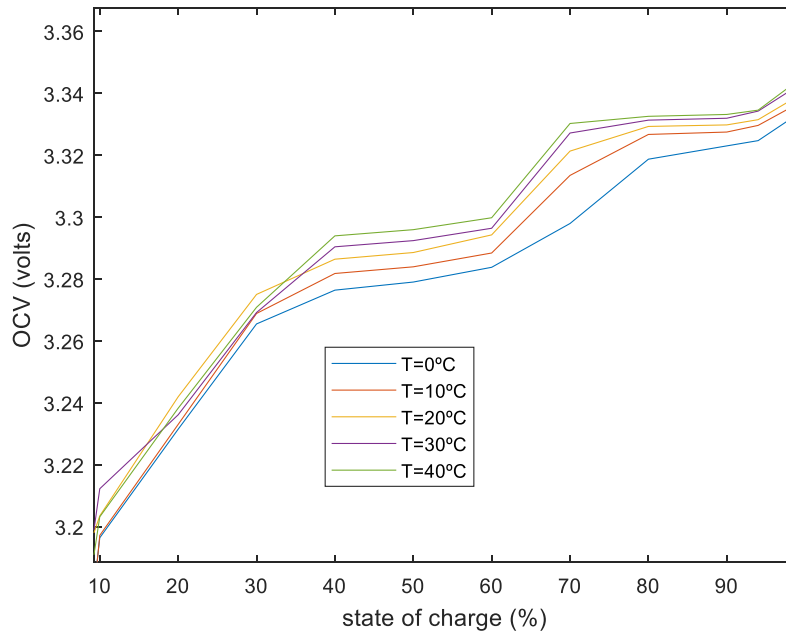
Figure 3-15 OCV at different temperature

Cell Impedance Parameters:

From the estimated results, it is difficult to draw a conclusion about the trend of the parameter values as a function of SOC or current. This is because the objective of the estimation algorithm is to minimize the sum squared error of the cost function considering any combinations of the parameters. The only constraint is the parameters should positive since they represent physical electrical impedance elements. However, series resistance is higher at lower SOC level of the battery cell, specially SOC less than 10%. The value of R_0 also increase with the current value as a general trend. The estimated impedance parameters are shown from Figure 3-16 to Figure 3-22.
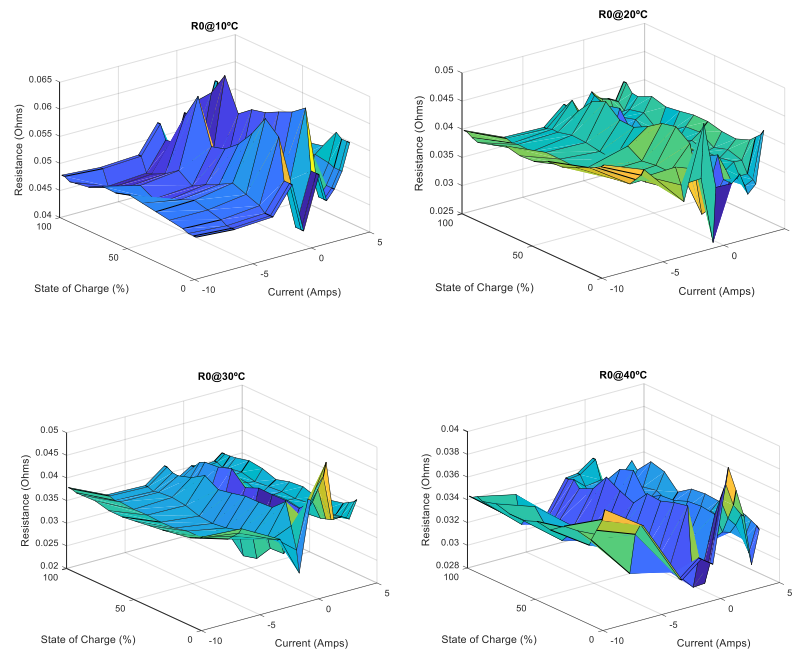
Figure 3-16 R_0 at different ambient temperature points
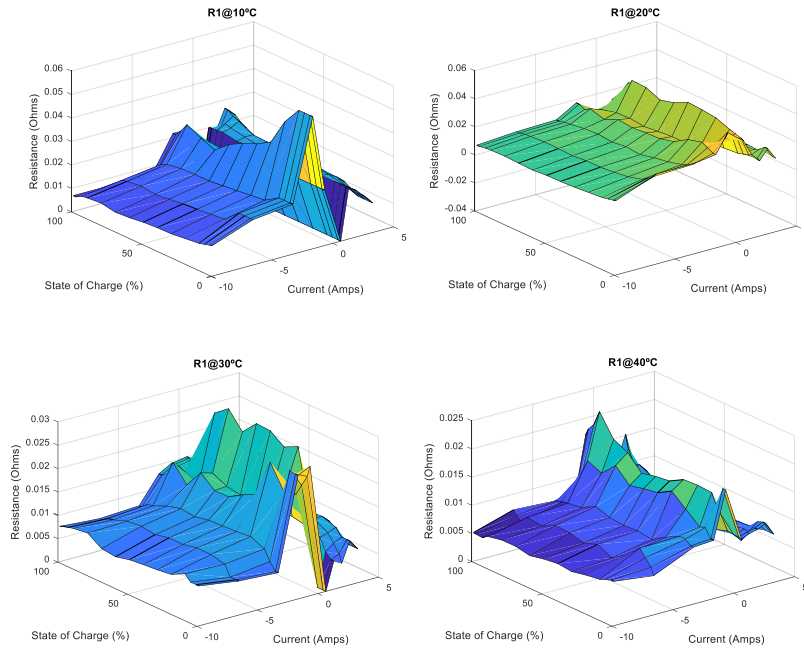
Figure 3-17 R_1 at different ambient temperature points
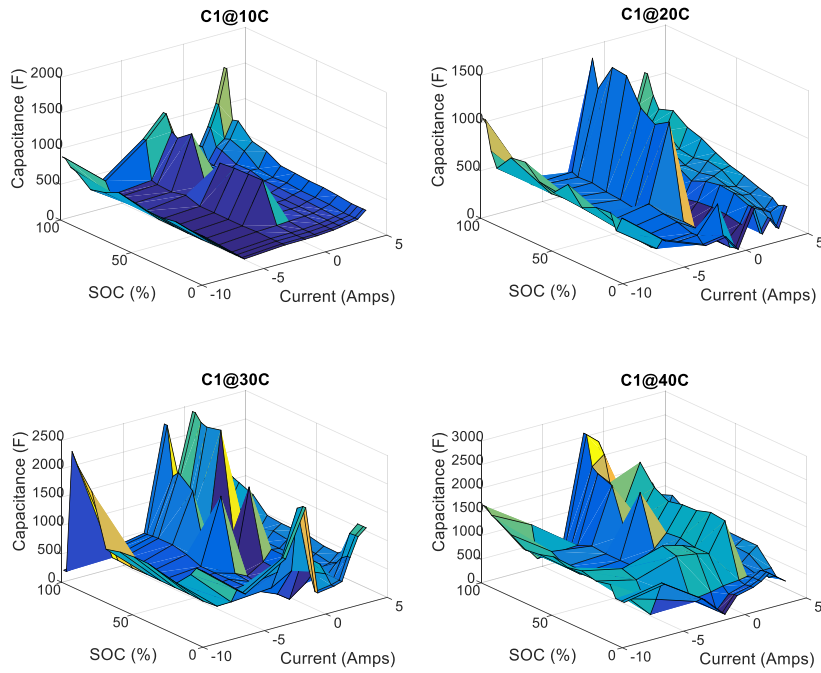
Figure 3-18 C_1 at different ambient temperature points
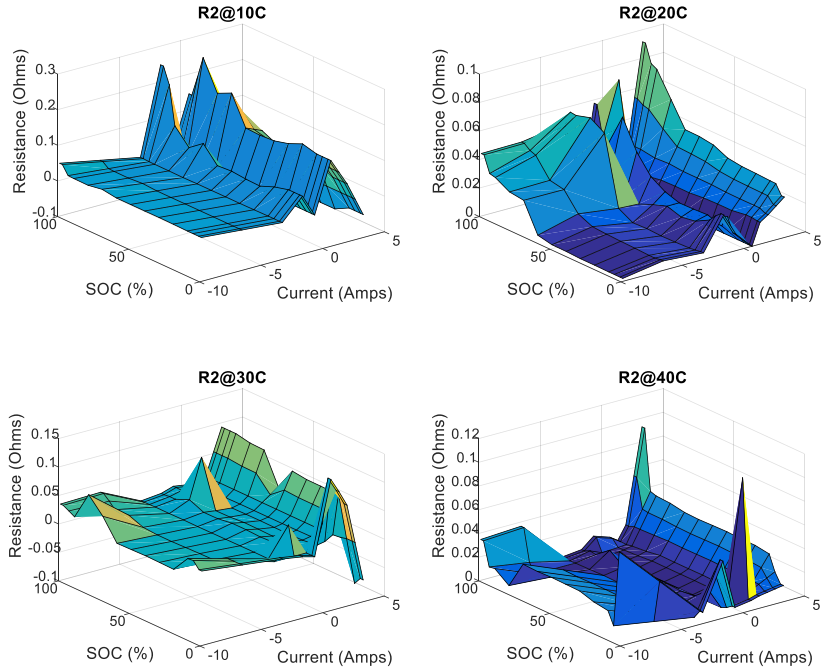
Figure 3-19 R_2 at different ambient temperature points
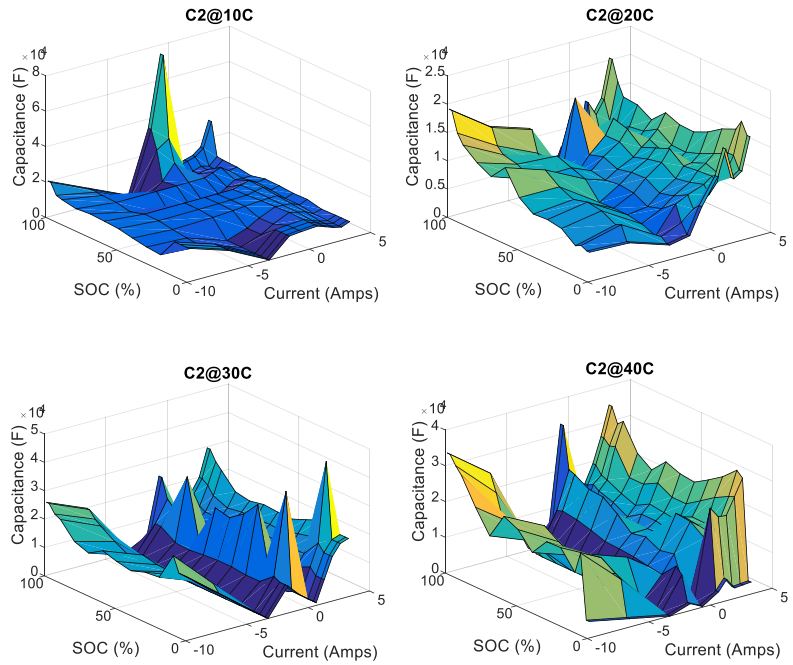
Figure 3-20 C_2 at different ambient temperature points

51
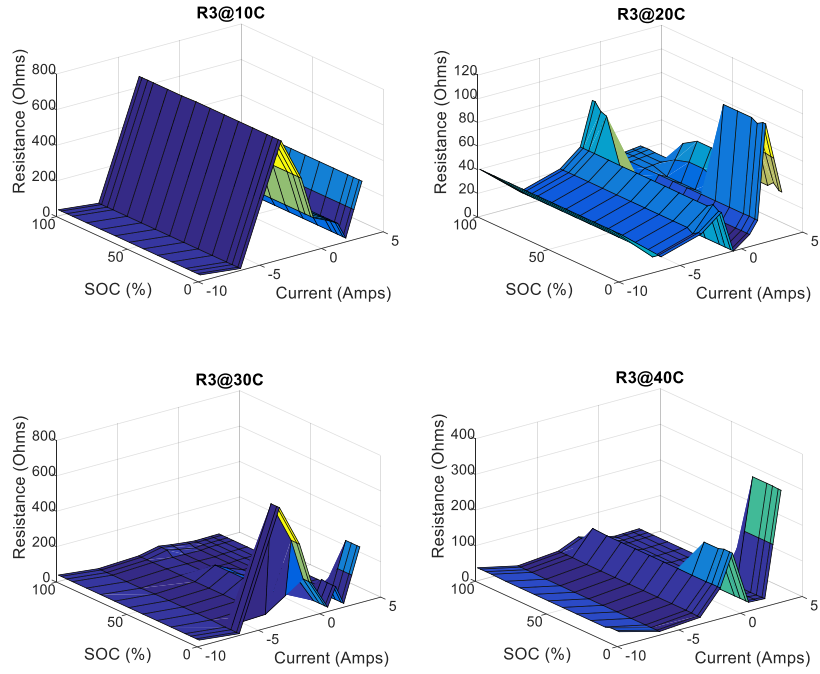
Figure 3-21 R_3 at different ambient temperature points
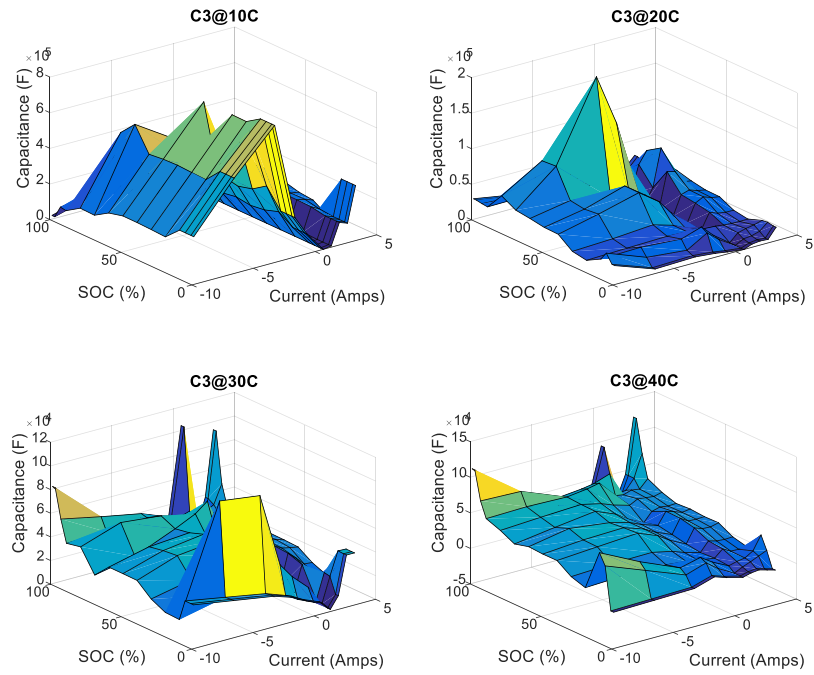
Figure 3-22 C_3 at different ambient temperature points

Chapter 4

Result and Discussion

In this chapter, model simulation results are compared with measured values and model performance is commented. The model is also validated using new experimental date from HPPC, DST and Pulse Discharge profiles.

4.1 Effect of SOC estimation, Number of model RC networks and temperature on terminal voltage

4.1.1   SOC Estimation Result for HPPC Profile

SOC is estimated using coulomb counting technique. Figure 4-1 shows the calculated SOC from the current profile and estimated from the measured current. The error between those two SOC is in Figure 4-2. The difference is high at the current transition points. It is partially the current shoots of charging/discharging device and the limitation in sampling rate. The error introduces proportional cell terminal voltage error since the model parameters depend on cell SOC.
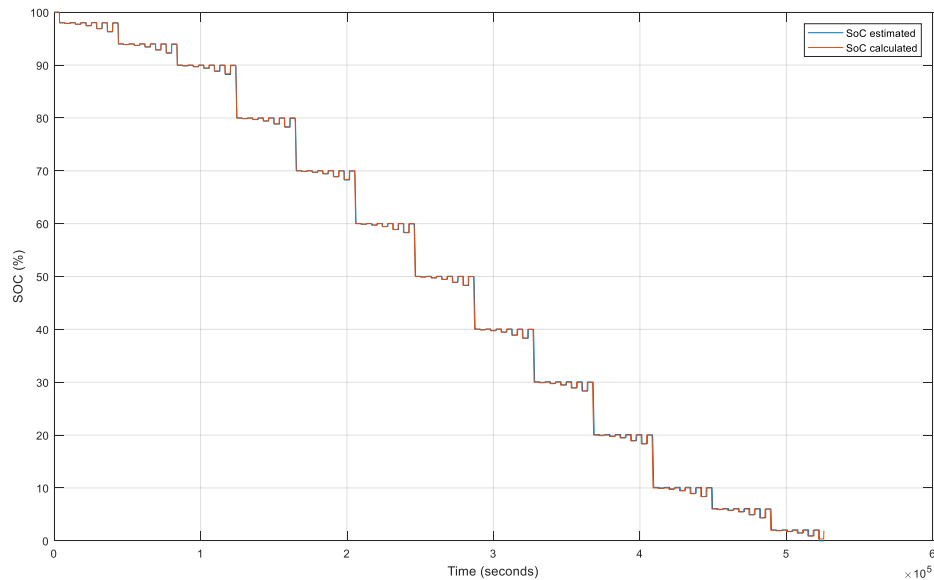
Figure 4-1 SOC estimated and calculated
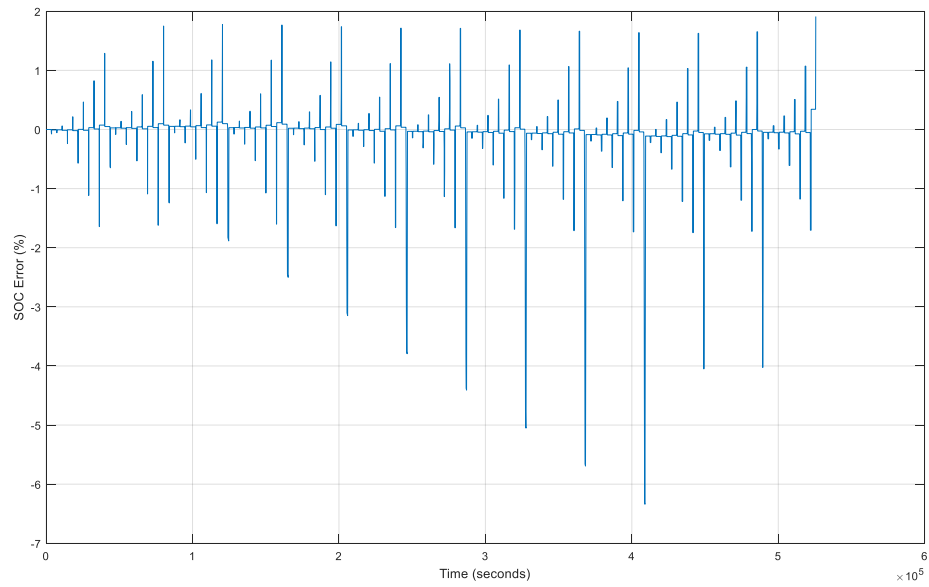
Figure 4-2 % SOC Error between estimated and calculated

4.1.2   **Number of RC Networks**

In Figure 4-3 measured voltage is compared with model simulated voltage with different number of RC networks. Model with 3RC network has good performance for both high and low frequency.
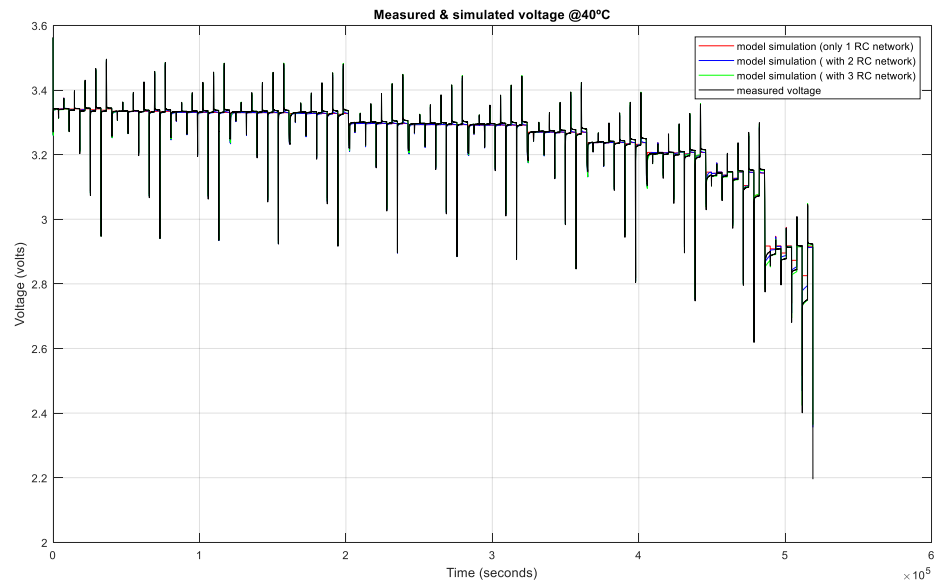
Figure 4-3 Measured & model simulated voltage with different number of RC networks at 40°C
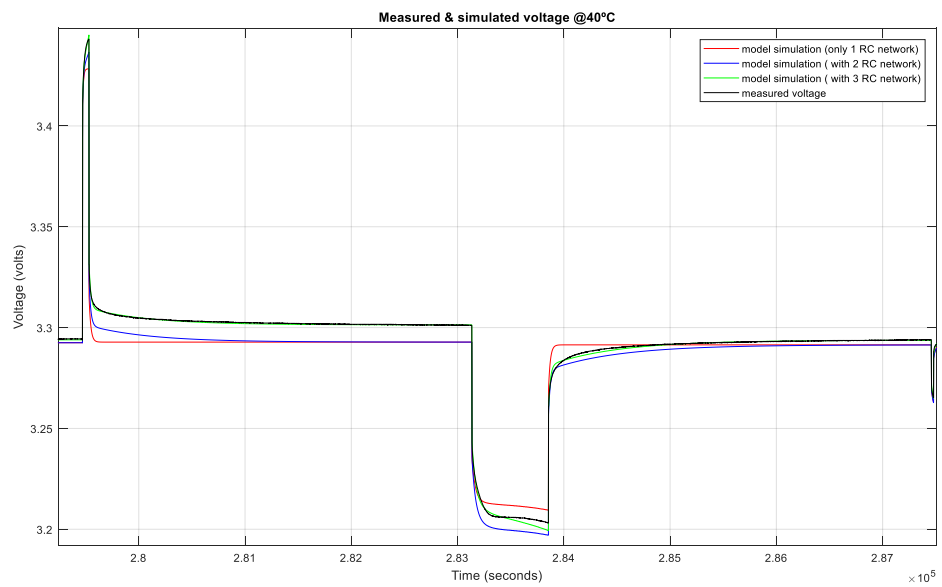
Figure 4-4 Measured & model simulated voltage with different number of RC networks at 40°C (zoomed)

55

4.1.3   **Temperature Effect**

Operating ambient temperature has effect on the cell terminal voltage. Both OCV and impedance parameters are affected by temperature. Figure 4-5 compared the measured terminal voltage at 40°C and Model simulation considering the ambient temperature far from 40°C. at it is shown in the figure considering working temperature in modelling improves the model performance well. At low SOC the effect is significant.
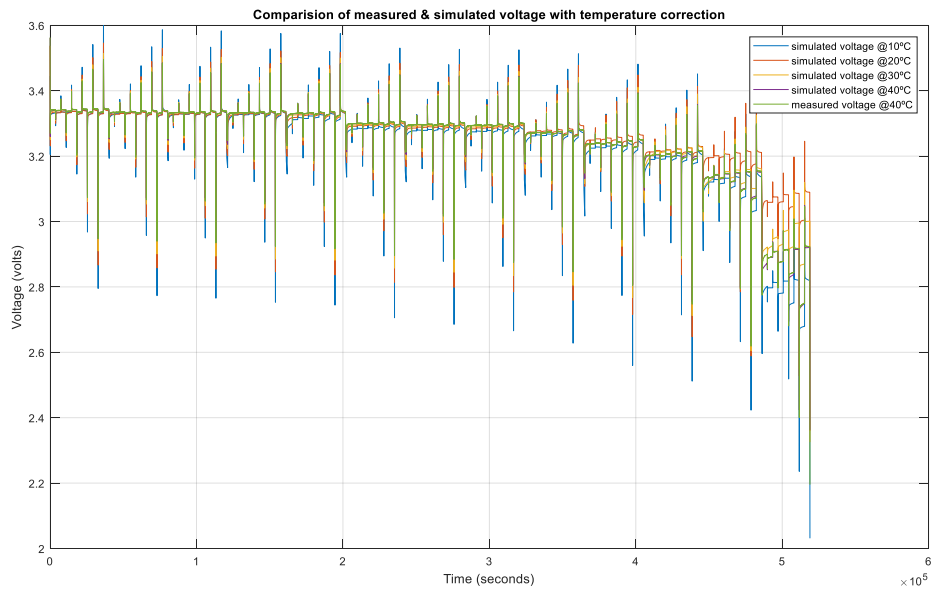
Figure 4-5 Effect of temperature correction on the model accuracy

Comparision of measured & simulated voltage with temperature correction

Legend:
- simulated voltage @10ºC
- simulated voltage @20ºC
- simulated voltage @30ºC
- simulated voltage @40ºC
- measured voltage @40ºC
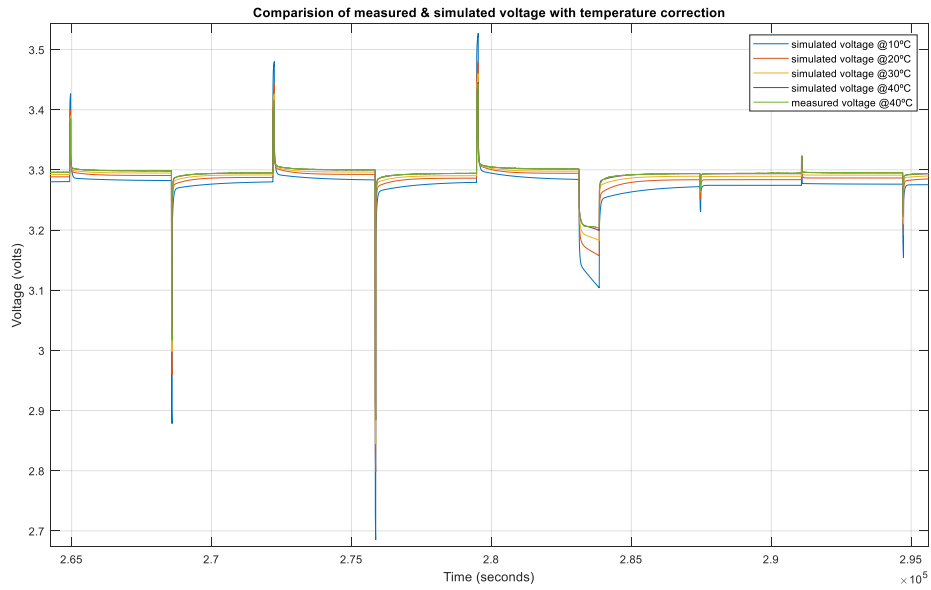
Figure 4-6 Effect of temperature correction on the model accuracy (zoomed)

4.2 Model and Measured Values Comparison

HPPC test data is compared with measured data at different temperature points from 98%-2% SOC range.

@Temperature = 10°C

Terminal voltage at 10ºC

Legend:
- Measured
- Estimated

57
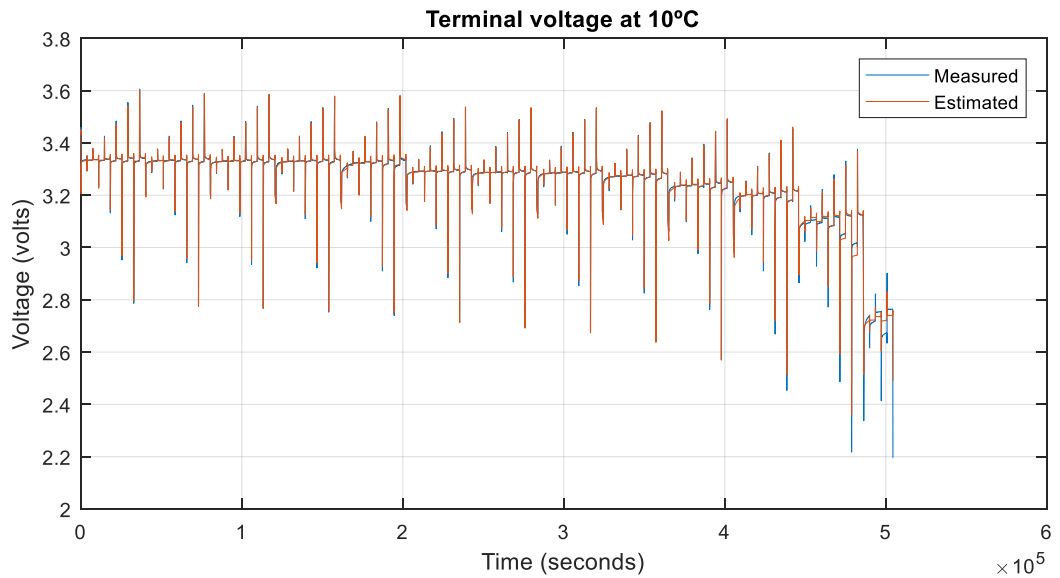
Figure 4-7 Measured and estimated terminal voltage at 10°C
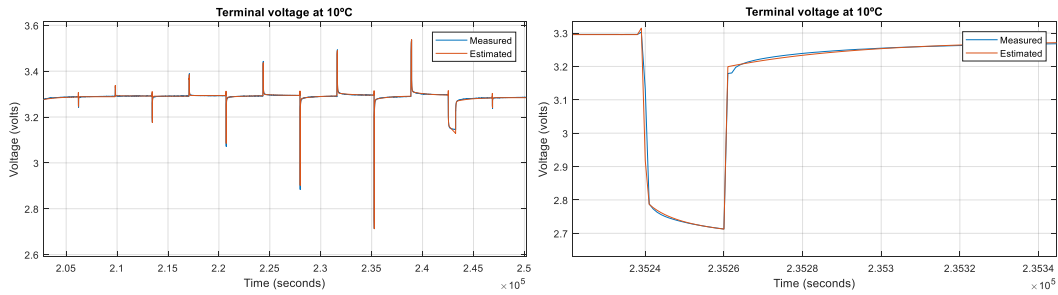
Figure 4-8 Measured and estimated terminal voltage at 10°C zoomed at 60% SOC (left) and 3C current rate (right)

The error between measured and model value is high at the current transient instants, however the mean sum squared error is lower than 10mv. The error also gets higher for SOC range less than 10%. This is because of the change in VOC in this range is higher. This error can be reduced by increasing the number of SOC breakpoints in the range.
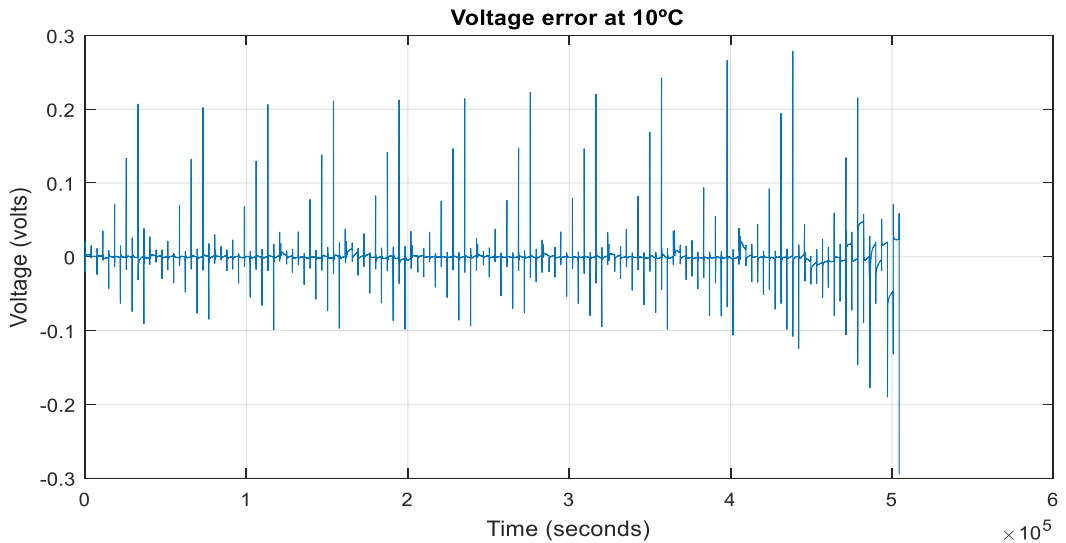
Figure 4-9 Voltage error at 10°C
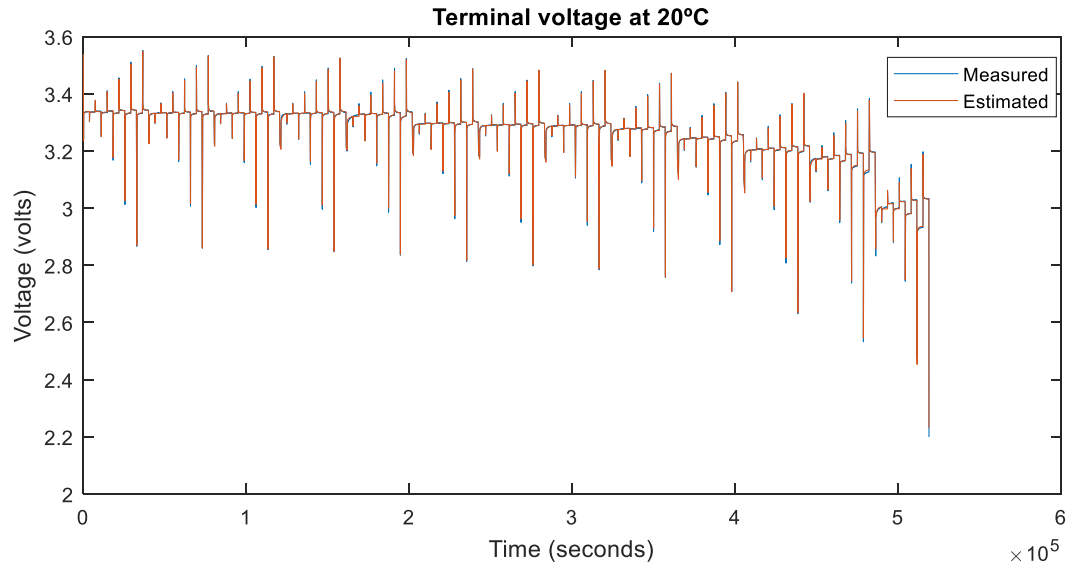
Figure 4-10 Measured and estimated terminal voltage at 20°C
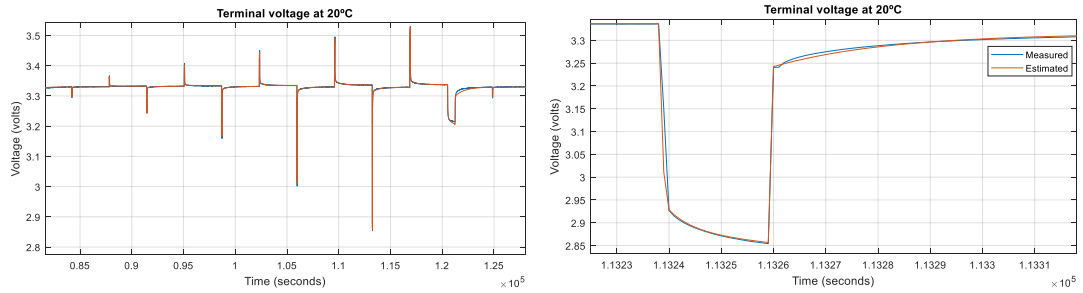
Figure 4-11 Measured and estimated terminal voltage at 20°C zoomed at 90% SOC (left) and 3C current rate (right)
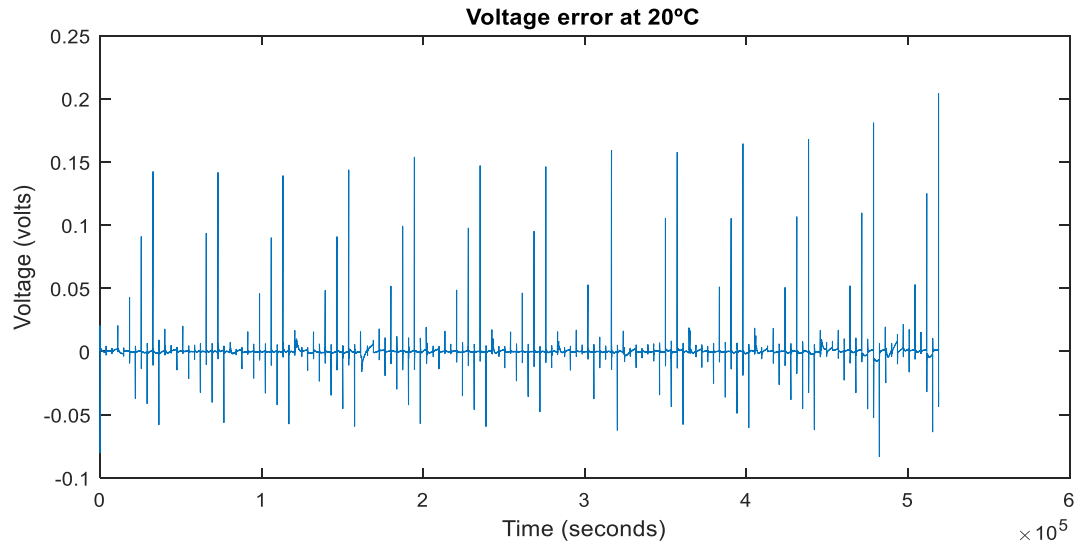
Figure 4-12 Voltage error at 20°C

@Temperature = 30°C
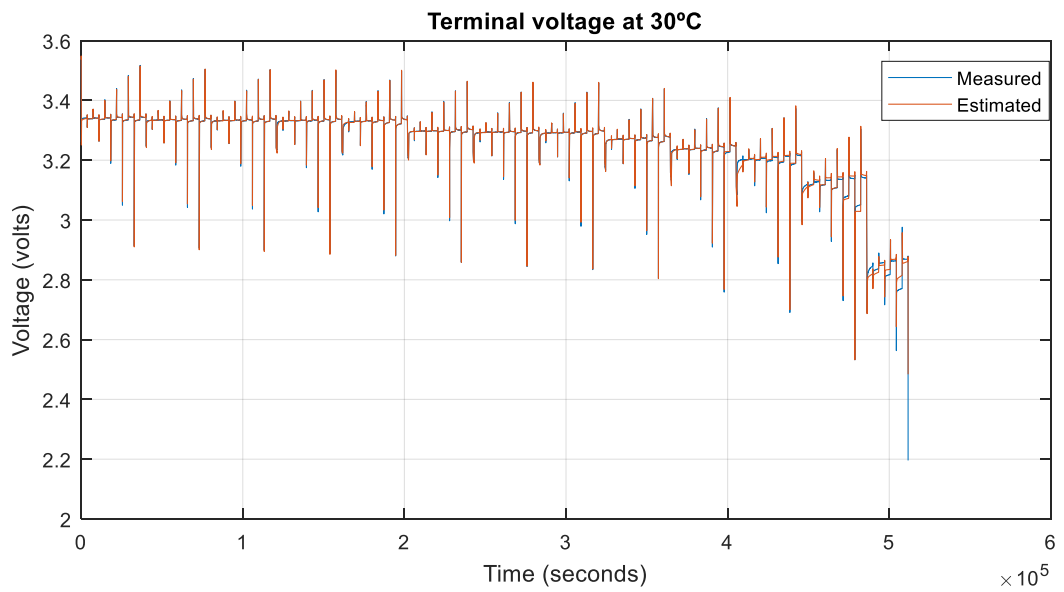
Figure 4-13 Measured and estimated terminal voltage at 30°C
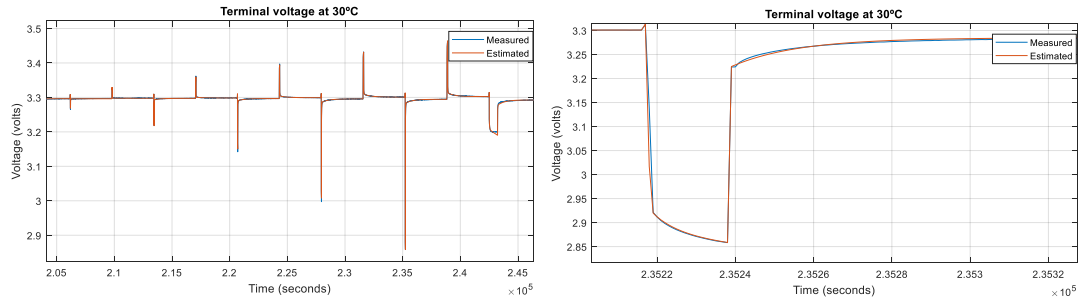
Figure 4-14 Measured and estimated terminal voltage at 30°C zoomed at 60% SOC (left) and 3C current rate (right)
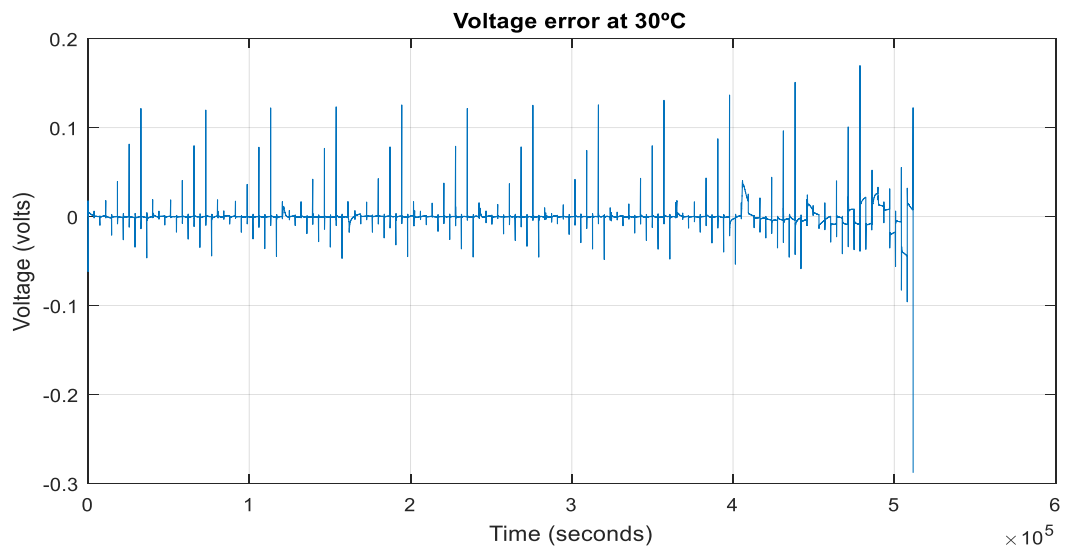
Figure 4-15 Voltage error at 30°C
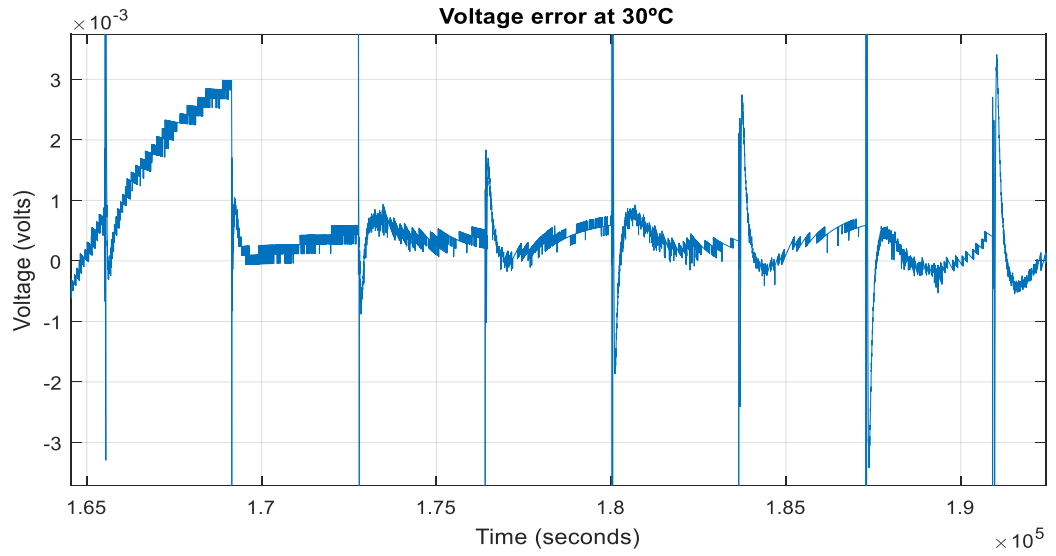
Figure 4-16 Voltage error at 30°C (zoomed)

@Temperature = 40°C
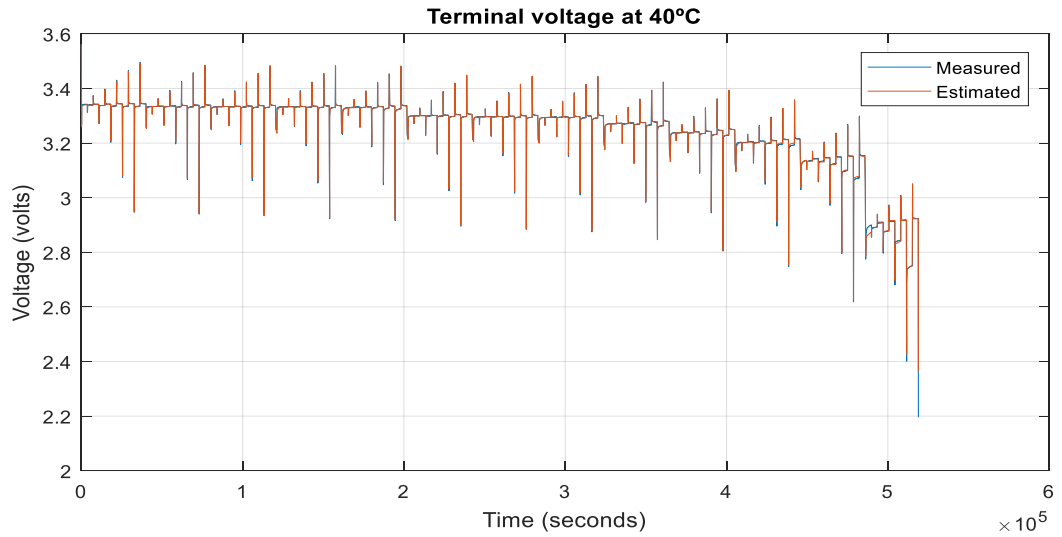
Figure 4-17 4-18Measured and estimated terminal voltage at 40°C
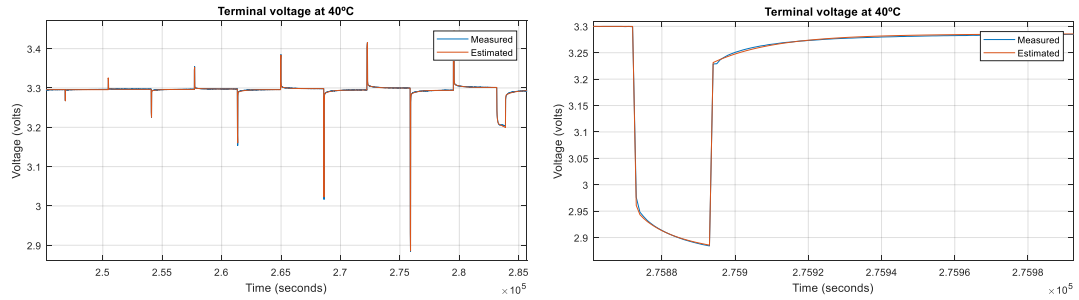
Figure 4-19 Measured and estimated terminal voltage at 40°C zoomed at 50% SOC (left) and 3C current rate (right)
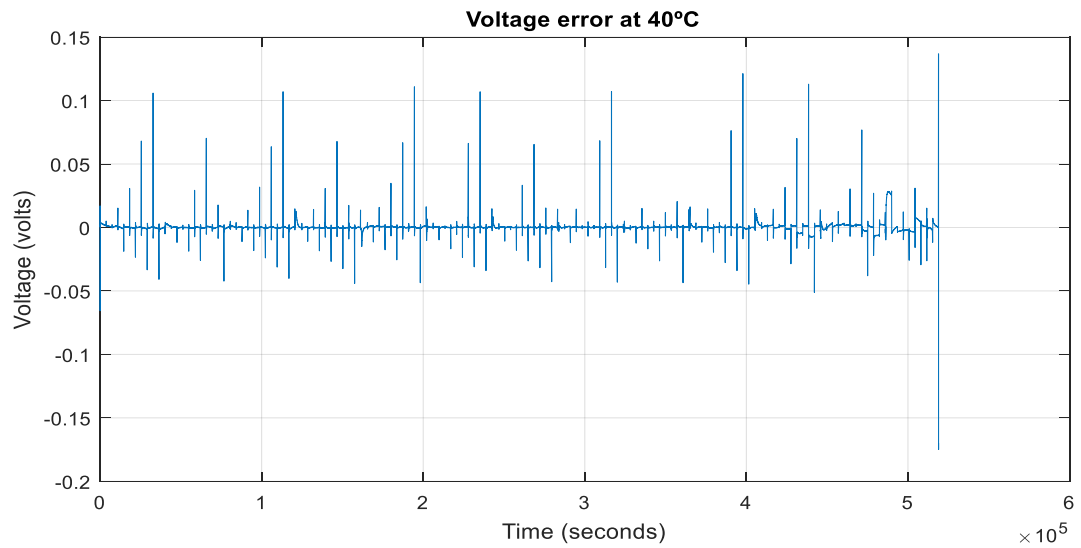
Figure 4-20 Voltage error at 40°C

4.3 Model Validation

The proposed model is validated with new measurement data from HPPC, DST and pulse discharge tests.

4.3.1 Hybrid pulse power characterization (HPPC)

A new HPPC test is done at 30C and the model validation result is shown in Figure 4-21 from 100% to 80% SOC.
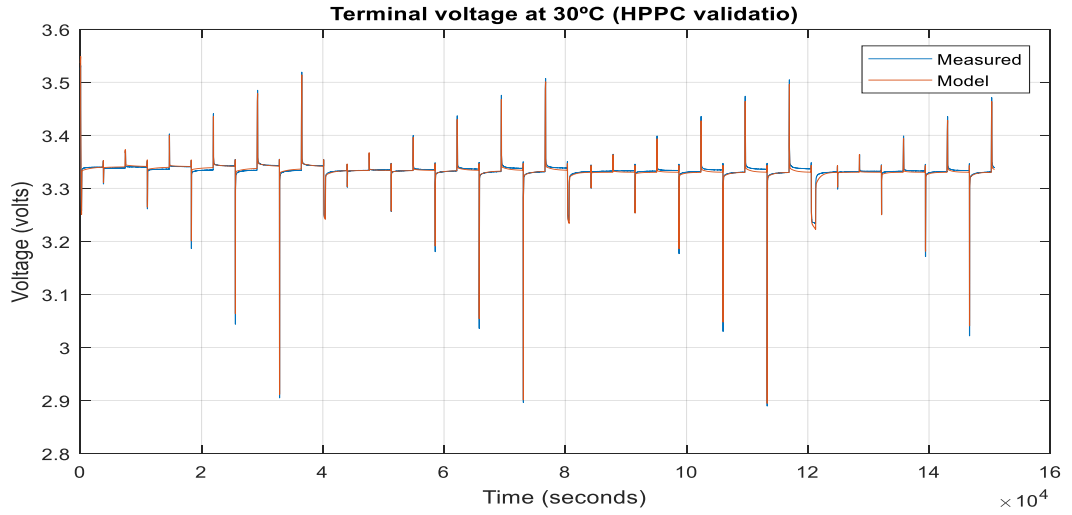
Figure 4-21 HPPC model validation at 30°C
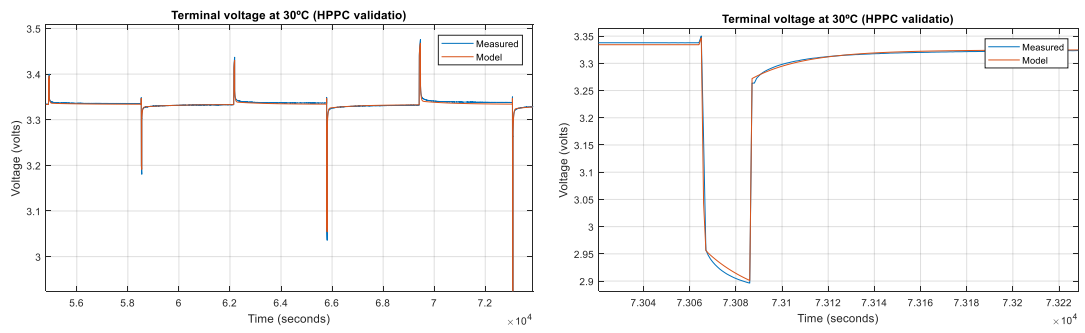
Figure 4-22 HPPC model validation at 30°C zoomed at 94% SOC (left) and at 3C current rate (right)
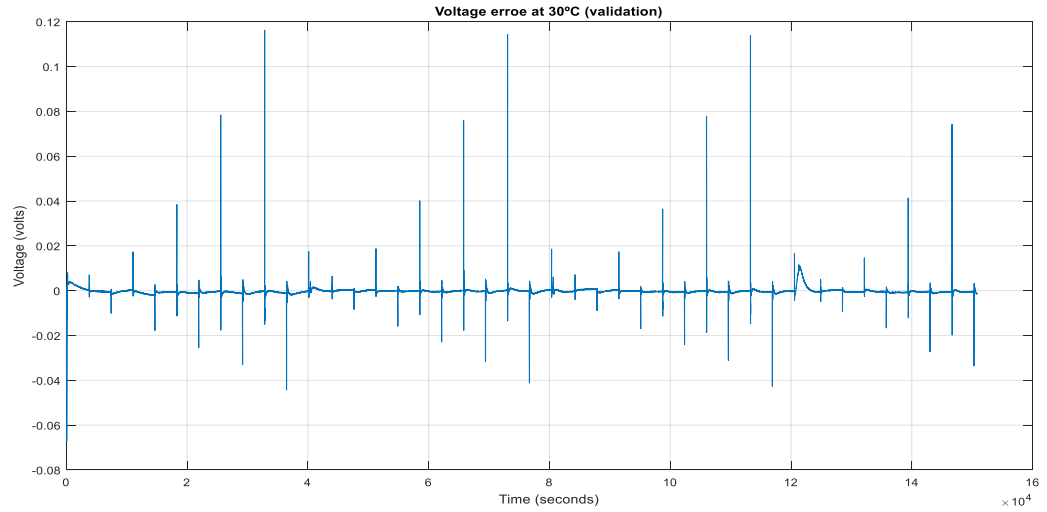
Figure 4-23 Voltage error for HPPC model validation at 30°C
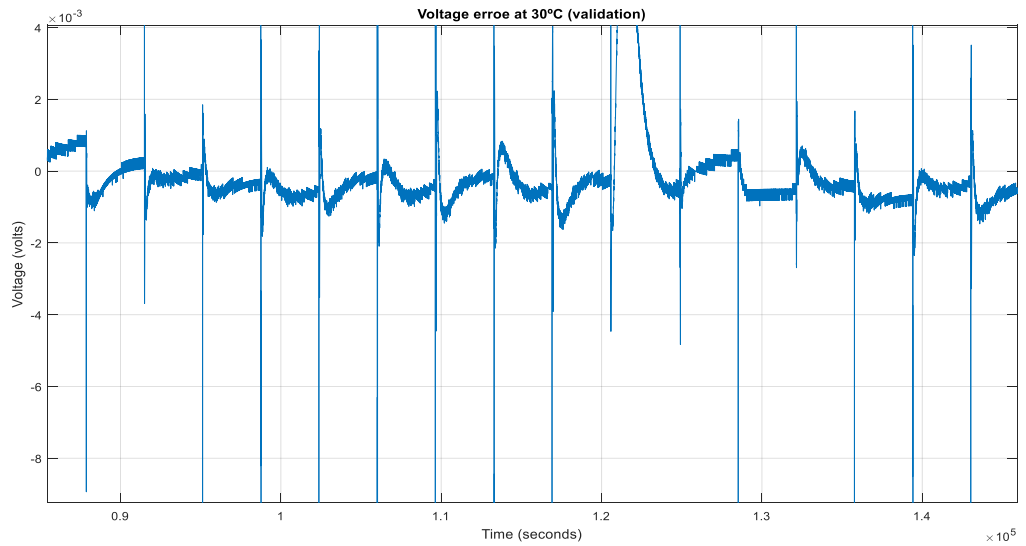
Figure 4-24 Voltage error for HPPC model validation at 30°C (zoomed)

4.3.2 **Dynamic Stress Test (DST)**

The model is tested with DST current profile shown in Figure 4-25 to validate the dynamic robustness of the model. Figure 4-25 shows customized current profile for validation and Figure 4-26 is measurement and model response for full discharge of the cell at 30°C. The model is also

validated with the same current profile at 35°C and 40°C. As it is shown from the figures below, the model performs good during validation except for low SOC of the cell.
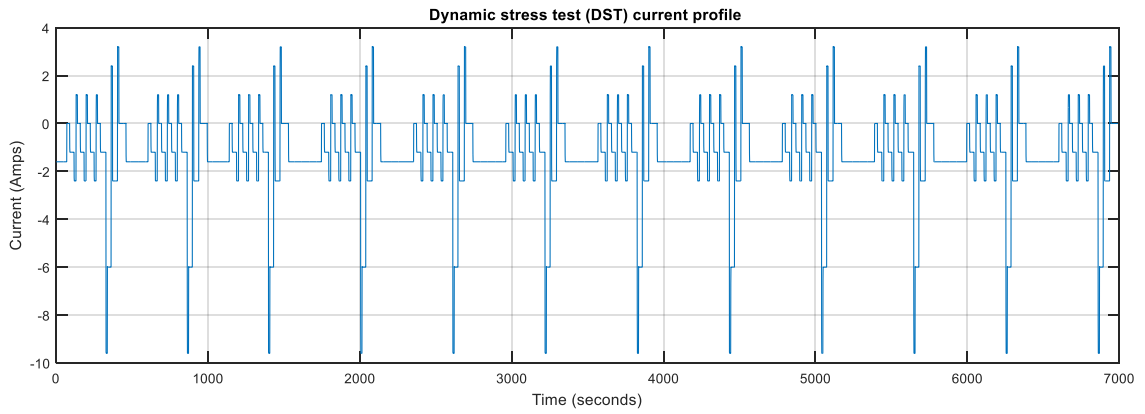
Figure 4-25 Customized DST current profile
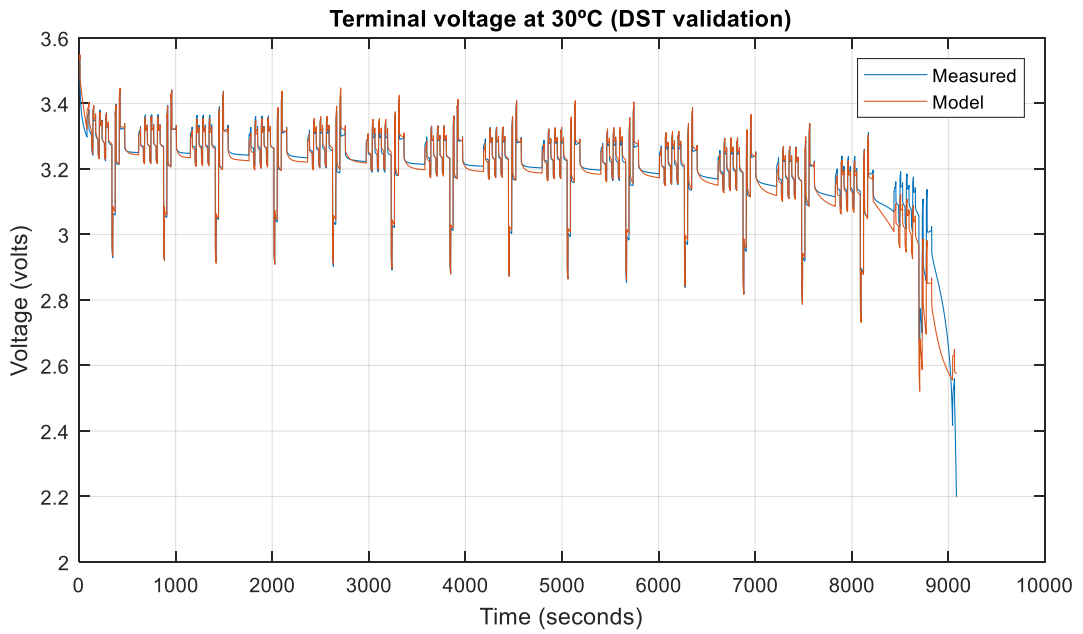
Figure 4-26 DST model validation at 30°C
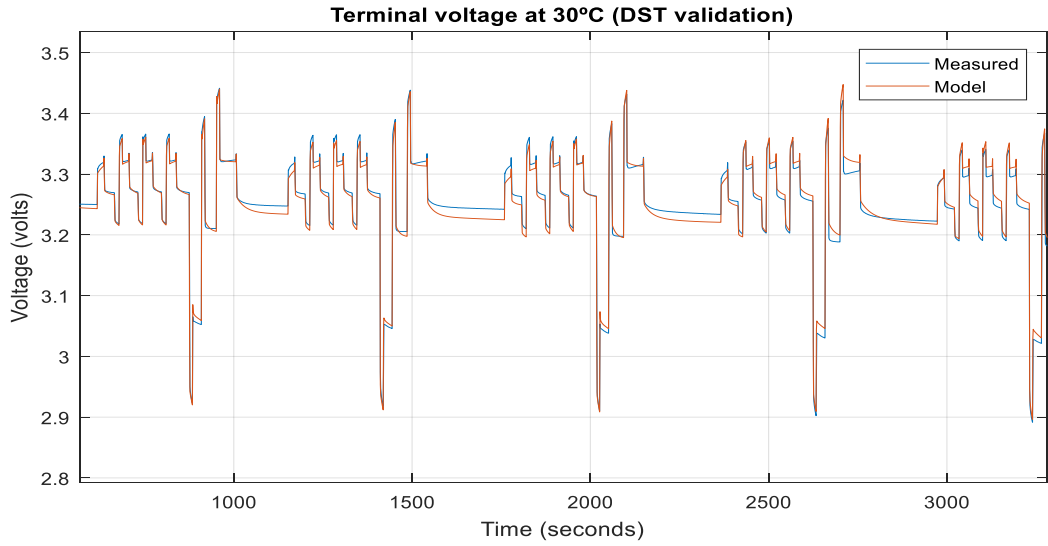
Figure 4-27 DST model validation at 30°C (zoomed)
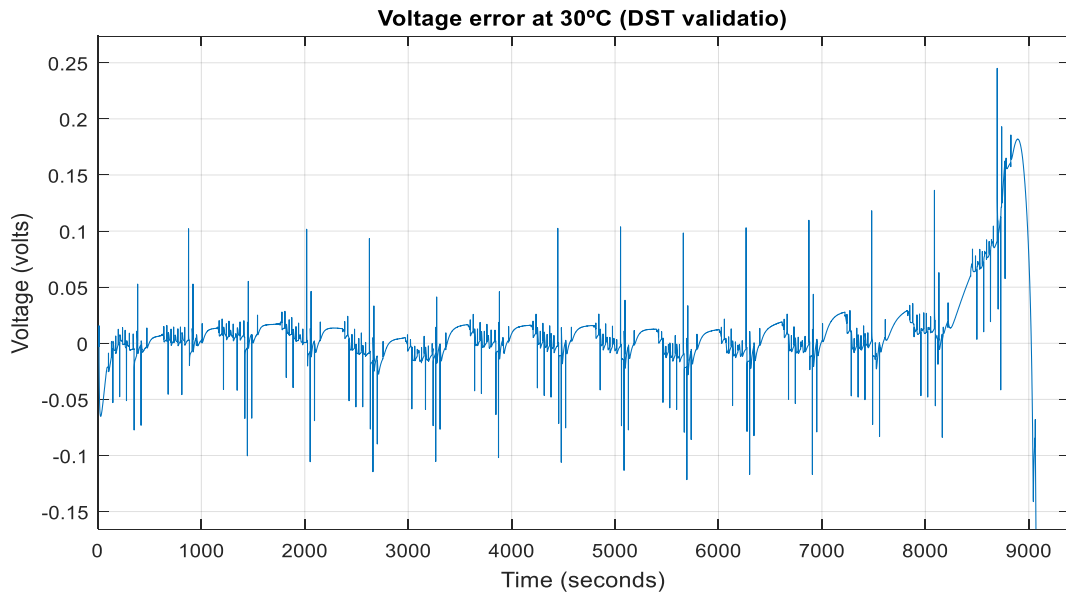
Figure 4-28 Voltage error for DST model validation at 30°C
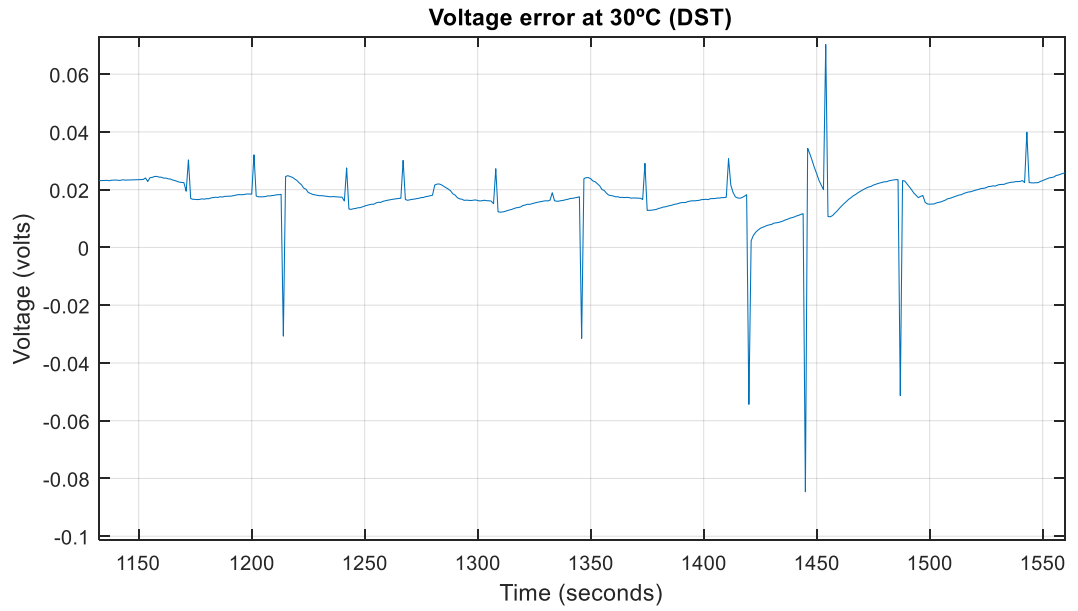
Figure 4-29 Voltage error for DST model validation at 30°C (zoomed)
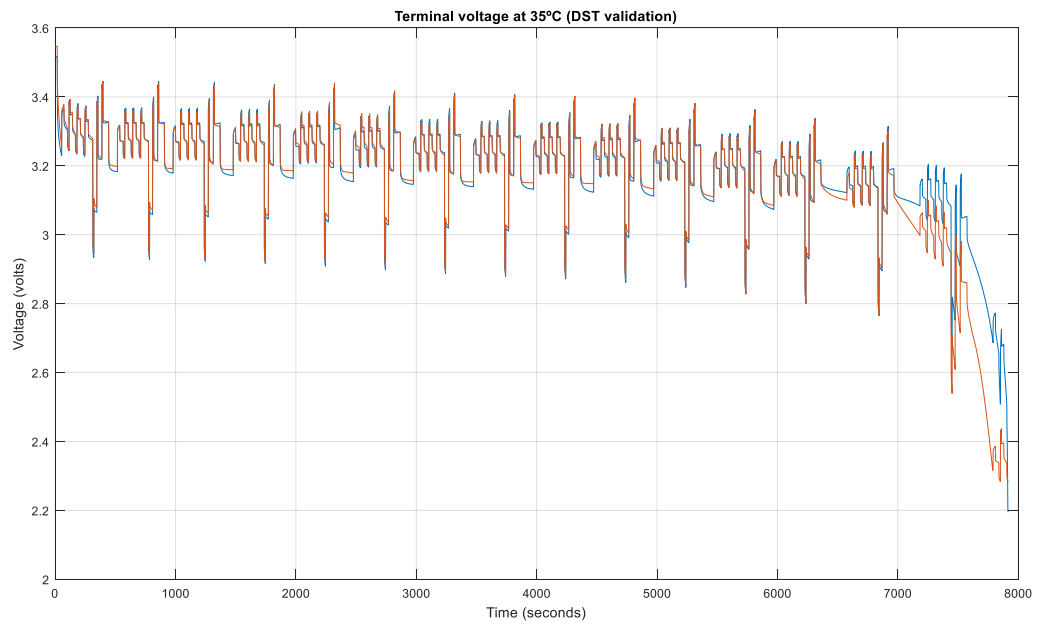
Figure 4-30 DST model validation at 35°C (100-0%SOC discharge)
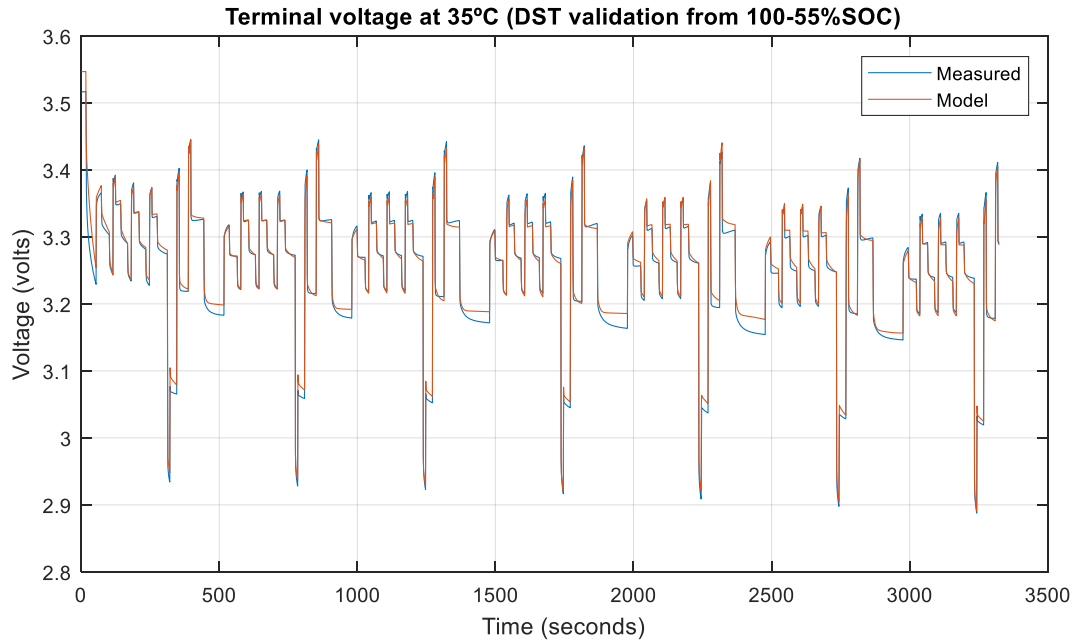
Figure 4-31 DST model validation at 35°C (100%-55%SOC discharge)
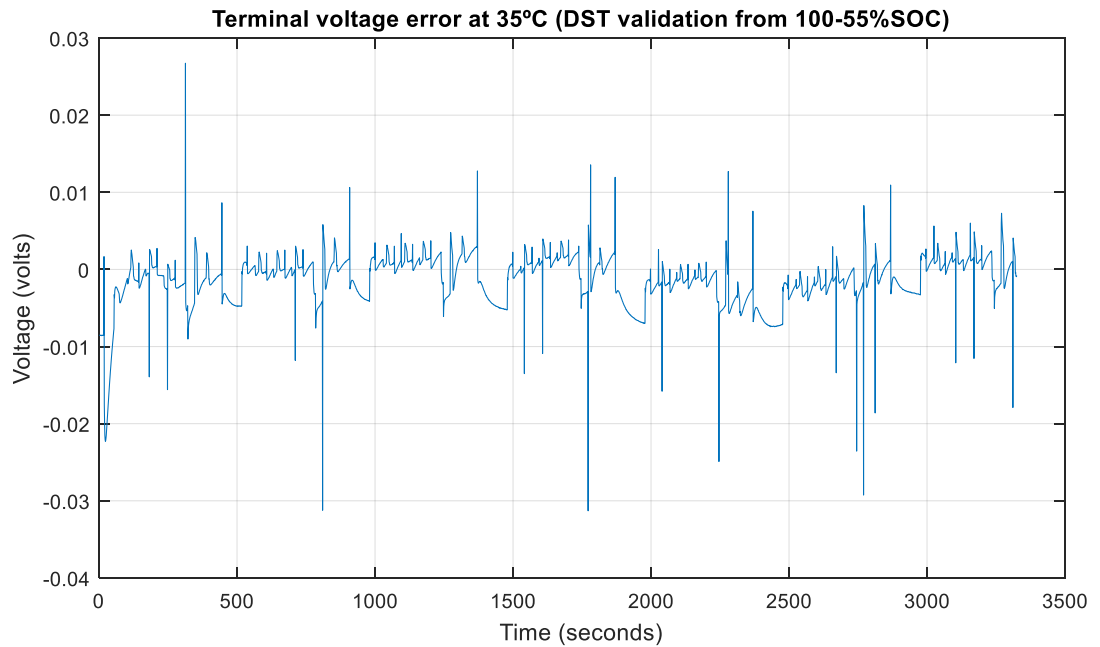
Figure 4-32 Voltage error for DST model validation at 35°C (100%-55%SOC discharge)

69
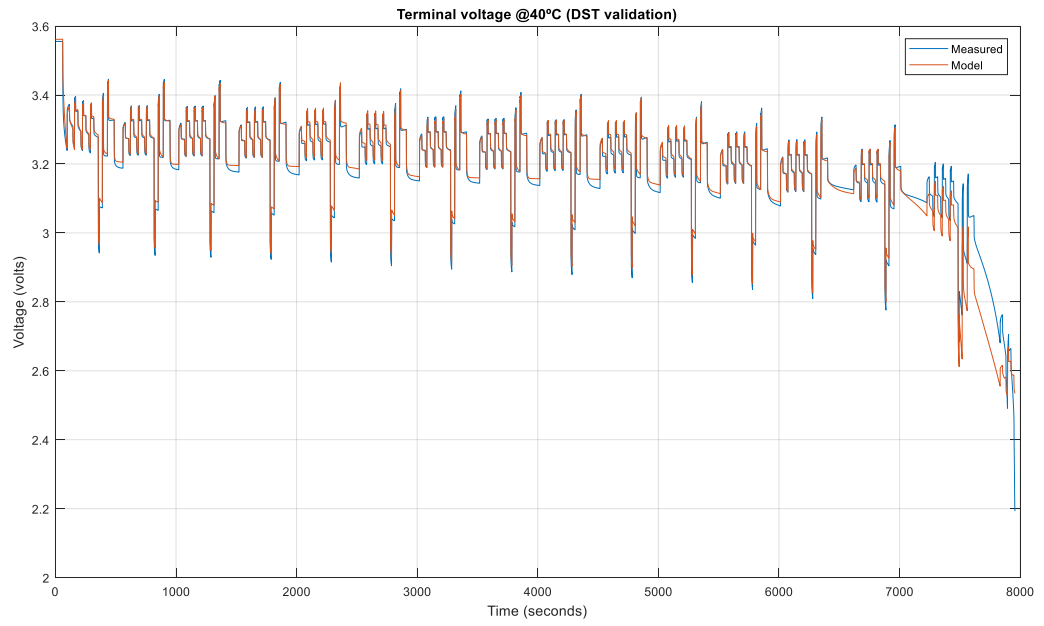
Figure 4-33 DST model validation at 40°C (100-0%SOC discharge)
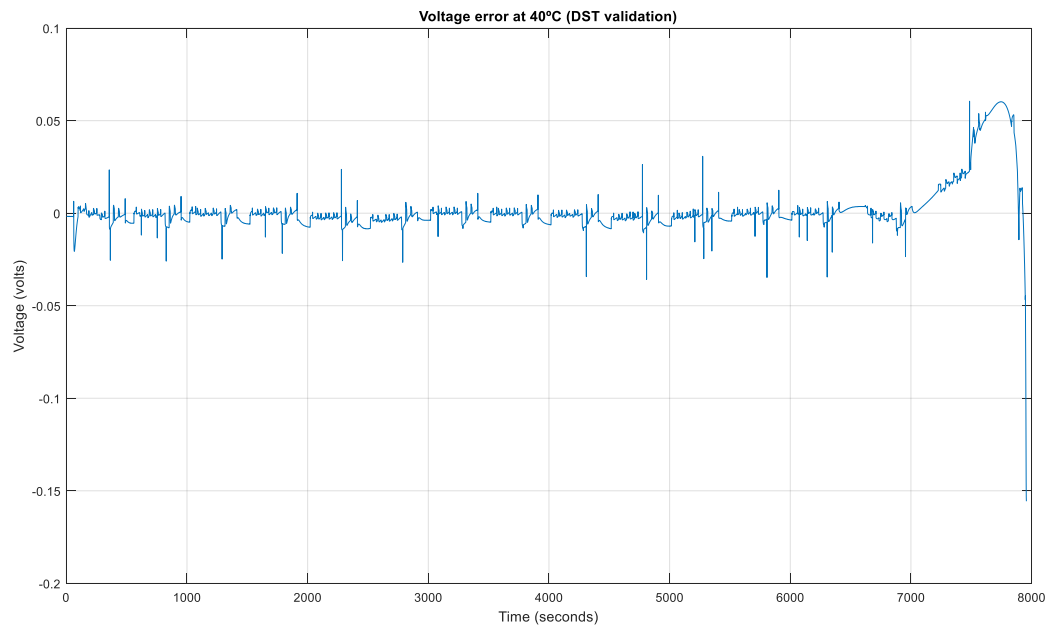
Figure 4-34 Voltage error for DST model validation at 40°C

70

4.3.3 Pulse Discharge

The model is also validated on pulse discharge currents shown in Figure 4-35 for fully discharge of the cell at 30C°.
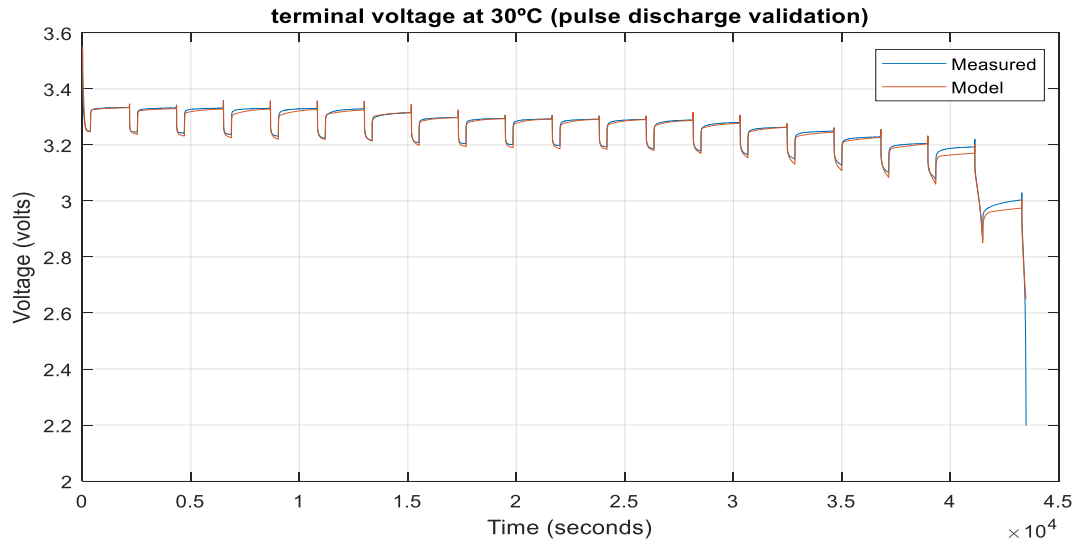
Figure 4-35 Pulse discharge model validation at 30°C
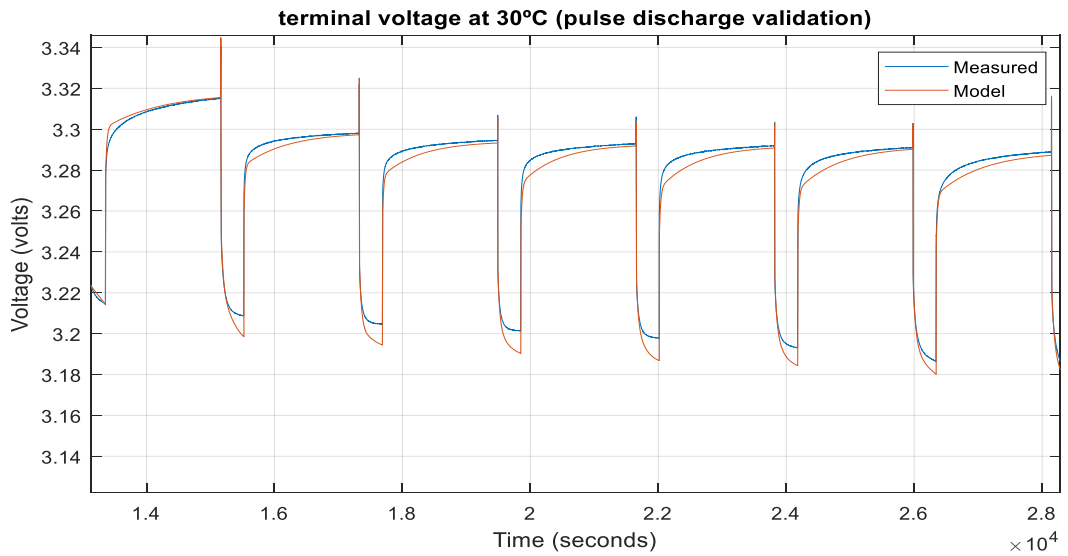
Figure 4-36 Pulse discharge model validation at 30°C (zoomed)
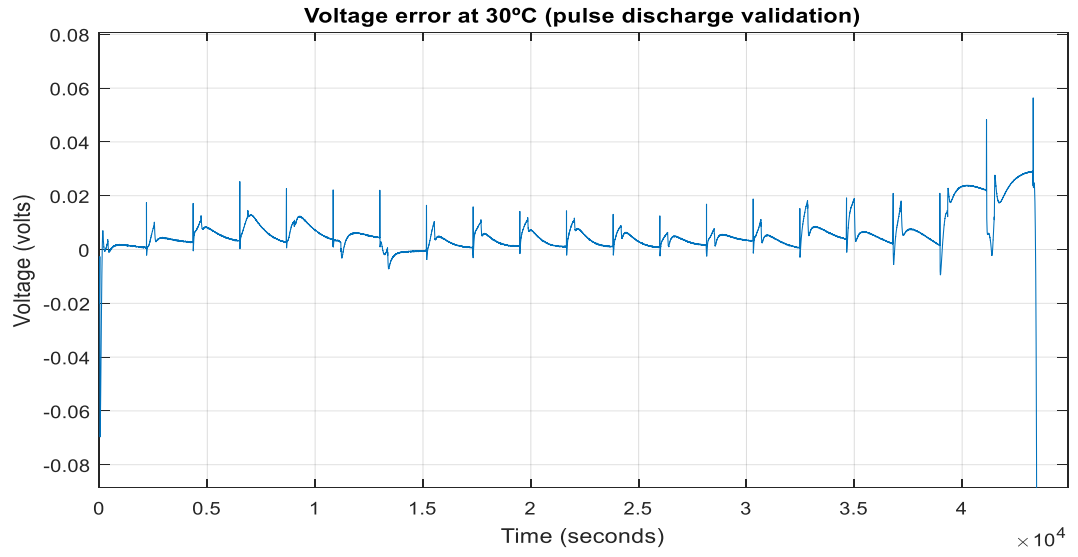
Figure 4-37 Voltage error for pulse discharge model validation at 30°C

Chapter 5

Conclusion and Future Work

5.1 Conclusion

In this thesis, MATLAB simulation model is developed for lithium ion battery cell based on experimental data. Hybrid pulse power characterization test is performed to collect data for parameter estimation. The model is an EEC which consists of a variable voltage source in series with a resister and three parallel RC networks. State of charge, temperature and current dependent impedance parameters are considered in the model. The model parameters are represented in lookup table form. MATLAB optimization toolbox is applied to estimate the final value of the parameters based on least square minimization techniques. The model is finally validated using dynamic stress and pulse discharge experimental tests. Simulink/Simscape based is lithium ion battery cell simulation model is developed as the main contribution of the work.

The focus of the work was developing temperature dependent battery cell model for pack and system level simulation. Lithium ion is now common in many applications as a power source from portable device to huge storage systems. The model can be used to simulate the performance of a lithium ion battery in various applications including hybrid power systems.

5.2 Future Work

The modelling approach implemented is empirical. Hence, the estimated parameters of the model are highly dependent on the quality of the experimental data. The performance and robustness of the model can be improved by exercising the battery well during experiment to capture the battery dynamics better. The way parameters estimated for the system is, the estimation is done for single SOC and temperature point with different cell current on charge and discharge. The parameters are collected to form full matrix. This is due to the limitation of estimating to many parameters with too much data points in the optimization toolbox. The accuracy of the model can be increased by estimating parameters at fixed charge-discharge current and temperature with full SOC range.

The model developed assumes the battery cells under experiment are 'new' which means that the they exercised only few numbers of cycles. However, as the number of cycles increase the electrical and thermal behavior of the battery cell changes. To consider this degradation effect in the model,

it needs lifetime experimental data of the cell. The experimental test to analyze the degradation effect of the cell usually needs long time. In the future work this effect will be included by performing the necessary experimental tests.

Bibliography

[1] P. GL., "Extended Kalman filtering for battery management systems of LiPB based Part 1," *Power Sources ,* vol. 134, no. 2, p. 252–261, 2004.

[2] H. G. B. C. Min Ye, "A model-based adaptive state of charge estimator for a lithium-ion battery using an improved adaptive particle filter," *Applied Energy ,* vol. 190, pp. 740-748, 2017.

[3] J. L. S. Y. J. Y. X. Z. Xi Zhang, "A novel method for identification of lithium-ion battery equivalent circuit model parameters considering electrochemical properties," *Journal of Power Sources ,* vol. 345 , pp. 21-29, 2017.

[4] R. X. H. H. Zhirun Li, "An improved battery on-line parameter identification and state-of-charge determining method," *Energy Procedia ,* vol. 103, p. 381 – 386, 2016 .

[5] N. W. C. C. M. P. Wei He, "State of charge estimation for Li-ion batteries using neural network modeling and unscented Kalman filter-based error cancellation," *Electrical Power and Energy Systems,* vol. 62, p. 783–791, 2014 .

[6] L. Y. Y. X. a. M. P. Ximing Cheng, "Novel Parametric Circuit Modeling for Li-Ion Batteries," *energies,* 14 July 2016.

[7] J. M. D. C. D. D. D. N. D. P. S. ,. D. H. K. a. D. C. N. Michael Knauff, "Simulink Model of a Lithium-Ion Battery for the Hybrid Power System Testbed".

[8] A. J. A. P. Y. K. N. R. N. I. Low Wen Yao, "Modeling of Lithium-Ion Battery Using MATLAB/Simulink," *IEEE,* Vols. 978-1-4799-0224-8/-13, 2013.

[9] C. S. C. W. L. W. 3. a. J. J. Zuchang Gao, "Integrated Equivalent Circuit and Thermal Model for Simulation of Temperature-Dependent LiFePO4 Battery in Actual Embedded Application," *energies,* no. 10, 85; doi:10.3390/en10010085, 11 January 2017.

[10] J. W. M. D. J. C. Xing Luo, "Overview of current development in electrical energy storage technologies and the application potential in power system operation," *Applied Energy,* vol. 137 , p. 511–536, 2015.

[11] S. M. L. E. G. L. G. F. J. M. C. Sergio Vazquez, "Energy Storage Systems for Transport and Grid Applications," *IEEE TRANSACTIONS ON INDUSTRIAL ELECTRONICS,* vol. 57, no. 12, pp. 3881-3895, DECEMBER 2010.

[12] I. S. a. J. L. S. Bruno G. Pollet, "Current status of hybrid, battery and fuel cell electric vehicles: From electrochemistry to market prospects," *Special Issue of Electrochimica Acta – International Year of Chemistry 2011 Electrochemical Science and Technology - State of the Art and Future Perspectives ,* December 2012.

[13] "European enviromenttal agency," 03 2014. [Online]. Available: https://europa.eu/european-union/topics/transport_en. [Accessed 09 08 2017].

[14] S. o. G. G. Emissions, "United states enviromental protection agency," 2015. [Online]. Available: https://www.epa.gov/ghgemissions/sources-greenhouse-gas-emissions. [Accessed 09 08 2017].

[15] S. T. H. T. E. P. Farhad Khosrojerdi, "Integration of Electric Vehicles into a Smart Power Grid: A Technical Review," *IEEE Electrical Power and Energy Conference (EPEC),* 2016.

[16] C. W. L. Y. W. a. K. S. Kwo Young, "Electric Vehicle Battery Technologies," in *Electric Vehicle Integration into Modern Power Networks, Power Electronics and Power Systems*, Springer Science+Business Media New York 2013, 2013, pp. 15-43.

[17] "Cegasa Portable energy," Cegasa Portable energy, [Online]. Available: http://www.cegasa.es/en/technology/lithium-ion. [Accessed 24 07 2017].

[18] J. M. J. XingLuo, "Overview of current development in electrical energy storage technologies and the application potential in power system operation," *Applied Energy,* vol. 137, pp. 511-536, 1 January 2015.

[19] A. G. ,. F. O. ,. F. V. M. Conte, "Hybrid battery-supercapacitor storage for an electric forklift:a life-cycle cost assessment," *J Appl Electrochem ,* vol. 44, pp. 523-532, 2014.

[20] H. L. TaoMa, "Development of hybrid battery–supercapacitor energy storage for remote area renewable energy systems," *Applied Energy,* vol. 153, pp. 56-62, 1 September 2015.

[21] S. C. I. Chotia, "Battery Storage and Hybrid Battery Supercapacitor Storage Systems: A Comparative Critical Review," *IEEE,* 2015.

[22] T. Horiba, "Lithium-Ion Battery Systems," *Proceedings of IEEE,* vol. 102, no. 6, pp. 939-950, June 2014.

[23] "Battery University," Battery University, 11 04 2016. [Online]. Available: http://batteryuniversity.com/learn/article/secondary_batteries. [Accessed 24 07 2017].

[24] T. F. F. a. J. N. Marc Doyle, "Modeling of Galvanostatic Charge and Discharge of the Lithium/Polymer/Insertion Cell," *The Electrochemical Society,* vol. 140, no. 6, pp. 1526-1533, January 12, 1993..

[25] J. L. ,. S. Y. ,. J. Y. ,. X. Z. Xi Zhang, "11. A novel method for identification of lithium-ion battery equivalent circuit model parameters considering electrochemical properties," *Journal of Power Sources ,* vol. 345, pp. 21-29, 2017.

[26] J. &. T. W. Newman, "Porous-Electrode Theory with Battery Applications," *AIChE Journal,* vol. 21, no. 10.1002/aic.690210103, pp. 25 - 41, 1975.

[27] 2. Shengbo Eben Li et al, "An electrochemistry based impedance model for lithium ion batteries," *journal of power sources.*

[28] W. G. a. C. Wang, "Thermal-electrochemical coupled modelling of lithium ion cell," *GATE Center for Advanced Energy Storage.*

[29] L. J. …. Shifei Yuan, "7. A transfer function type of simplified electrochemical model with modified boundary conditions and Pade approximations for Lithium ion battery, part 1 lithium concentration estimation.," *Journal of power system.*

[30] M. V. T. F. S. S. C. 3. Ngoc Tham Tran, "Matlab simulation of Lithium ion cell Using Electrochemical Sinngle particle Model," *Journal of power system.*

[31] s. A. Bizeray, "4. Advanced battery manegment system using fast electrochemical modelling," in *hybrid and electric vehicle conference ,* 2013.

[32] L. J. ,. C. Y. H. W. X. Z. Shifei Yuana, "10. A transfer function type of simplified electrochemical model with modified boundary conditions and Padé approximation for Li-ion battery: Part 2. Modeling and parameter estimation," *Journal of Power Sources,* vol. 352, p. 258–271, June 2017.

[33] R. X. a. J. F. Hongwen He, "Evaluation of Lithium-Ion Battery Equivalent Circuit Models for State of Charge Estimation by an Experimental Approach," *Energies ,* vol. 4, no. 10.3390/en4040582 , pp. 582-598, 2011.

[34] H. Y. a. W. G. 2Feng Jin, "Comparison Study of Equivalent Circuit Model of Li-Ion Battery for Electrical Vehicles," *Maxwell Scientific Organization,* vol. 6, no. 20, pp. 3756-3759, 2013.

[35] Y. &. T. T.-F. &. Q. D.-T. &. H. M.-H. Yang, "PNGV equivalent circuit model and SOC estimation algorithm of lithium batteries for electric vehicle. Xitong Fangzhen Xuebao," *Journal of System Simulation,* vol. 24, pp. 938-942, 2012.

[36] "Battery University," Battery University, 31 07 2017. [Online]. Available: http://batteryuniversity.com/learn/article/charging_at_high_and_low_temperatures. [Accessed 2017 08 2017].

[37] S. Zhang, K. Xu and T. Jow, "The low temperature performance of Li-ion batteries," *J.ournal of Power system,* vol. 115, p. 137–140, 2003.

[38] P. Mahamud.R, "Reciprocating air flow for Li-ion battery thermal management to improve temperature uniformity," *Journal of Power Sources,* vol. 196 , p. 5685–5696., 2011.

[39] E. G. D. ElenaMarkevich, "On the performance of graphitized meso carbon microbeads (MCMB)–meso carbon fibers (MCF) and synthetic graphite electrodes at elevated temperatures," *Journal of Power Sources,* vol. 174, no. 2, pp. 1263-1269, 6 December 2007.

[40] G. F. K. K. M. S. C. S. R. F. F. U. S. K. Patricia Handel, "Thermal aging of electrolytes used in lithium-ion batteries – An investigation of the impact of protic impurities and different housing materials," *Journal of Power Sources,* vol. 267, pp. 255-259, 1 December 2014.

[41] W. &. S. Van Schalkwijk, "Advances in Lithium-Ion Batteries," Springer, New York 2002, p. 47–68.

[42] C. M. T. &. M. P. Feng Leng, "Effect of Temperature on the Aging rate of Li Ion Battery Operating above Room Temperature," *Scientific Reports,* no. 12967 , 06 August 2015.

[43] B. S. a. M. Biju, "Theoretical Modelling Methods for Thermal Management of batteries," *Energies ,* vol. 8, no. doi:10.3390/en80910153, pp. 10153-10177, 2015.

[44] J. V. S. E. A. S. J. &. M. T. Barreras, "Datasheet-based modeling of Li-Ion batteries," in *IEEE Vehicle Power and Propulsion Conference*, Seoul: IEEE Press, 2012.

[45] C. a. t. U. o. Maryland, "Calce Battery Group," Center for Advanced Life Cycle Engineering, 2016. [Online]. Available: http://www.calce.umd.edu/batteries/testing.htm. [Accessed 25 07 2017].

[46] "Basics of Electrochemical Impedance Spectroscopy," Garmy Instruments, [Online]. Available: https://www.gamry.com/application-notes/EIS/basics-of-electrochemical-impedance-spectroscopy/. [Accessed 31 07 2017].

[47] G. Instruments, "Slideshare," 10 6 2015. [Online]. Available: https://www.slideshare.net/GamryInstruments/basics-of-electrochemical-impedance-spectroscopy. [Accessed 26 8 2017].

[48] A. S. f. E. E. a. R. E. (EERE), "Battery Test Manual for Electric Vehicles," U.S. Department of Energy Vehicle Technologies Program, June 2015.

[49] A. a. B. I. Hussein, "An Overview of Generic Battery Models," in *Proceedings of the IEEE Power and Energy Society General Meeting*, San Diego, July 2011.

[50] A. A. Hussein, "13. Kalman Filters versus Neural Networks in Battery State-of-Charge Estimation: A Comparative Study," *International Journal of Modern Nonlinear Theory and Application,* vol. 3, p. 199-209, 2014.

[51] *Instruction manual.* [Performance]. BaSyTech, 2016.

[52] Y.-x. Yuan, "15. A review of trust region algorithms for optimization," State Key Laboratory of Scientific and Engineering Computing, Institute of Computational Mathematics and Scientific/Engineering Computing, Chinese Academy of Sciences, P. O. Box 27, Beijing 100080, China.

[53] Mathworks, "Optimization Toolbox User's Guide," Mathworks, Natick, 2017.

[54] R. K. J. C. J. A. a. A. K. N. A. Chaturvedi, "5. Algorithms for Advanced Battery-Management Systems," *IEEE Control Systems,* vol. vol. 30, no. 3, pp. 49-68, June 2010.

[55] H. H. a. F. S. Weiwei Huo, "6. Electrochemical–thermal modeling for a ternary lithium ion battery during discharging and driving cycle testing," *RSC Adv,* pp. 57599-57607, 5 2015.

[56] U. W. F. L. M. K. Uwe Westerhoff, "Analysis of Lithium-Ion Battery Models Based on Electrochemical Impedance Spectroscopy," *Energy Technology,* vol. 4, no. 12, p. 1620–1630, August 2016.

[57] W. Z. G. L. Xiaoqiang Zhang, "9. A Review of Li-ion Battery Equivalent Circuit Models," *TRANSACTIONS ON ELECTRICAL AND ELECTRONIC MATERIALS,* vol. 17, no. 6, pp. 311-316, December 25, 2016.

[58] M. F. S. H. Mohammed Faraga, "12. Continuous piecewise-linear, reduced-order electrochemical model for lithium-ion batteries in real-time applications," *Journal of Power Sources,* vol. 342, p. 351–362, 28 February 2017.

[59] H. P. Gavin, "14. The Levenberg-Marquardt method for nonlinear least squares curve-fitting problems," Department of Civil and Environmental Engineering Duke University, March 22, 2017.

[60] "Lithium-Ion Batteries for Off-Grid Systems," [Online]. Available: https://www.homepower.com/articles/solar-electricity/equipment-products/lithium-ion-batteries-grid-systems. [Accessed 23 July 2017].

[61] L. B. A. R. a. M. C. Simone Orcioni, "Lithium-ion Battery Electrothermal Model, Parameter Estimation, and Simulation Environment," *Energies,* vol. 10, no. 375, pp. 1-20, 2017.

Appendix A

LFP Battery Cell Technical Specifications
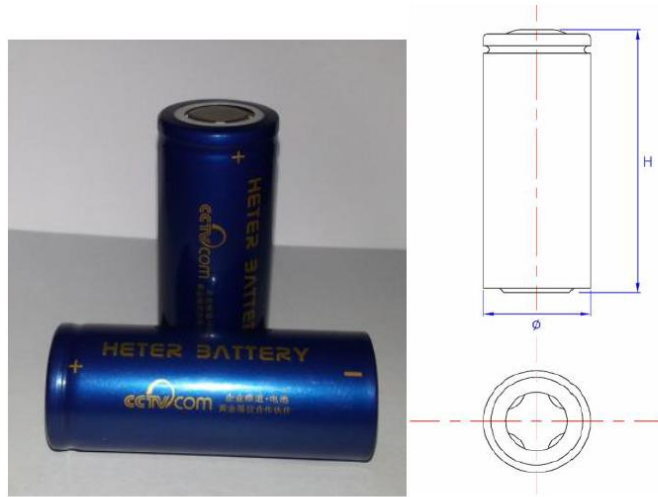
Item	Dimension (mm)
Diameter(Φ)	26.2±0.1
Height(H)	65.6±0.4

Figure 7-1 Cell appearance and dimension

No.	Item		Standard	Note
1	Standard Capacity		3200mAh	0.5C,(current value of 3200mA at 1C）
2	Capacity Range		3100~3300mAh	0.5C
3	Standard Voltage		3.2 V	
4	Alternating Internal Resistance		≤30mΩ	with PTC
5	Charge Conditions	Cut-off Voltage	3.65±0.05V	constant current charge to 3.65V at 0.5C, constant voltage charge to stop until 0.01C mA
		Cut-off Current	0.01C	
6	DischargeCut-off Voltage		2.5V	
7	Cycle Characteristic		2000 times	100% DOD, the residual capacity is no less than 80% of rated capacity at 1C rate.
8	Max. Continuous Discharge Current		9.6A	
9	Pulse Discharge Current		15A, 5s	
10	Working Temperature		Charge:0°C~55°C Discharge:-20°C~60°C	
11	Storage Temperature		-20°C ~ 45°C	
12	Battery Weight		86 g (Approx.)	

Figure 7-2 Battery cell major technical parameters

List of Tables

List of Figures

85

88

List of Abbreviations

BMS   Battery Management System

BSS   Battery Storage Systems

CAES   Compressed Air Energy Storage

DST   Dynamic Stress Test

ECM   Electrochemical Model

EEC   Electrical Equivalent Circuit

EES   Energy Storage System

EIS   Electrochemical Impedance Spectroscopy

EV   Electric Vehicle

HEV   Hybrid Electric Vehicle

HPPC   Hybrid Pulse Power Characterization

OCV   Open Circuit Voltage

PHS   Pumped Hydro Storage

RC   Resister-Capacitor

SMES   Superconducting Magnetic Energy Storage

SOC   State of Charge